

# C-H Bond-Making and -Breaking Processes in Heteronuclear Monoazadienyl Complexes: Reactivity of $\text{HFeRu}(\text{CO})_5\{\text{RC}=\text{C}(\text{H})\text{C}(\text{H})=\text{N}-i\text{Pr}\}$ toward $\text{CO}^1$

Olaf C. P. Beers and Cornelis J. Elsevier\*

Anorganisch Chemisch Laboratorium, Universiteit van Amsterdam, Nieuwe Achtergracht 166, 1018 WV Amsterdam, The Netherlands

Huib Kooijman, Wilberth J. J. Smeets, and Anthony L. Spek

Bijvoet Center for Biomolecular Research, Vakgroep Kristal- en Structuurchemie, Universiteit Utrecht, Padualaan 8, 3584 CH Utrecht, The Netherlands

Received November 9, 1992

In the photochemically induced reaction of  $\text{Ru}_2(\text{CO})_6\{\text{RC}=\text{C}(\text{H})\text{CH}_2\text{N}-i\text{Pr}\}$  (**1a**, R = Ph; **1b**, R = Me) with  $\text{Fe}_2(\text{CO})_9$  the heteronuclear complex  $\text{HFeRu}(\text{CO})_5\{\text{RC}=\text{C}(\text{H})\text{C}(\text{H})=\text{N}-i\text{Pr}\}$  (**5**) is formed in 35% yield.  $\text{HRu}_2(\text{CO})_6\{\text{RC}=\text{C}(\text{H})\text{C}(\text{H})=\text{N}-i\text{Pr}\}$  (**4**), which is prepared quantitatively by photolysis of  $\text{H}_2\text{Ru}_4(\text{CO})_8\{\text{RC}=\text{C}(\text{H})\text{C}(\text{H})=\text{N}-i\text{Pr}\}_2$  under a CO atmosphere, can act as an intermediate in this reaction and is proposed to be formed from **1** by a  $\beta$ -H-elimination reaction. Complex **5** is most likely formed via oxidative addition of the Ru-H bond in **4** to a  $\text{Fe}(\text{CO})_4$  fragment. Complex **5** reacts with CO at 293 K to give reductive elimination of the monoazadiene ligand and formation of  $\text{Fe}(\text{CO})_5/\text{Ru}_3(\text{CO})_{12}$ , probably via a mechanism involving opening of the hydride bridge. In the reaction of **5** with CO at 373 K the hydride is shifted to the monoazadienyl (MAD-yl) ligand, which is reduced from formally monoanionic to dianionic. In the case of R = Ph selective hydride transfer to  $\text{C}_\beta$  is observed, resulting in the formation of  $\text{FeRu}(\text{CO})_6\{\text{PhC}(\text{H})\text{C}(\text{H})\text{C}(\text{H})\text{N}-i\text{Pr}\}$  (**6a**), which features an unprecedented coordination mode of the MAD-yl ligand. For R = Me, both transfer to  $\text{C}_\beta$  (affording **6b**) and to  $\text{C}_{im}$  is observed, the latter affording  $\text{FeRu}(\text{CO})_6\{\text{MeC}=\text{C}(\text{H})\text{CH}_2\text{N}-i\text{Pr}\}$  (**7**). This R-group dependence and also the difference in the reactivity of **5** and its homonuclear  $\text{Ru}_2$  analogue **2** is rationalized by the strength of the  $\pi$ -C=C coordination in the intermediate  $\text{HFeRu}(\text{CO})_6\{\text{RC}=\text{C}(\text{H})\text{C}(\text{H})=\text{N}-i\text{Pr}\}$  (**9**). Complex **9a** could not be prepared by the reaction of  $[\text{FeRu}(\text{CO})_6\{\text{PhC}=\text{C}(\text{H})\text{C}(\text{H})=\text{N}-i\text{Pr}\}][\text{BF}_4]$  (**8a**) with  $\text{NaBH}_4$ , which afforded one diastereomer of  $\text{FeRu}(\text{CO})_6\{\text{PhCC}(\text{H})\text{C}(\text{H})\text{N}(\text{H})-i\text{Pr}\}$  (**10a**), but **9a** was formed by the conversion of **8a** on silica. The X-ray crystal structures of **6a** and **9a** have been determined. Crystals of **6a** are monoclinic, space group  $P2_1/c$ , with unit-cell dimensions  $a = 12.106(14)$  Å,  $b = 9.490(10)$  Å,  $c = 16.780(7)$  Å,  $\beta = 97.61(7)^\circ$ ,  $V = 1911(3)$  Å<sup>3</sup>,  $Z = 4$ , final  $R = 0.055$ , and  $R_w = 0.040$  for 2215 reflections with  $I > 3.0\sigma(I)$  and 245 parameters. Crystals of **9a** are orthorhombic, space group  $P2_12_12_1$ , with  $a = 9.819(1)$  Å,  $b = 11.928(1)$  Å,  $c = 17.338(1)$  Å,  $V = 2030.7(3)$  Å<sup>3</sup>,  $Z = 4$ , and final  $R = 0.044$  for 1434 reflections with  $I > 2.5\sigma(I)$  and 254 parameters. The most important conclusion of this work is that isostructural FeRu- and  $\text{Ru}_2$ -MAD-yl complexes show a large difference in reactivity, which can be rationalized by stronger  $\pi$ -coordination of the MAD-yl ligand to Fe as compared to Ru.

## Introduction

Very few systematic studies are known in which the reactivity of coordinated hydrocarbons in isostructural homo- and heteronuclear complexes has been compared. One example concerns the reactivity of  $\text{FeRu}(\text{CO})_4\text{Cp}_2$ ,<sup>2a</sup> and it was found that in reaction with alkynes this heteronuclear system closely resembles the homonuclear diiron system, but it is more reactive than either of the homodinuclear parent compounds. In another study, the reactivity of  $\text{MM}'(\text{CO})_6\{\text{RN}=\text{C}(\text{H})\text{C}(\text{H})=\text{NR}\}$  ( $\text{MM}' = \text{FeFe}, \text{FeRu}, \text{RuRu}$ ) toward alkynes showed a considerable

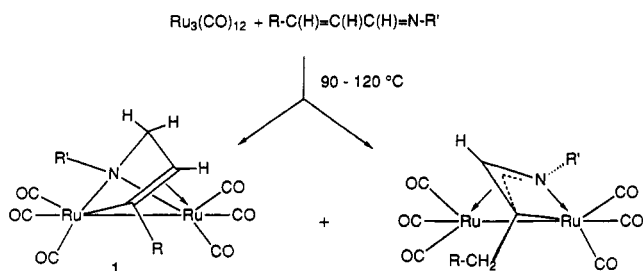
influence of the type of metal core.<sup>2b</sup> In this case the results were explained by the proposal of two different initial reaction steps for each of the homodinuclear analogues, while the product formation with the heteronuclear complex showed features of both of the homonuclear analogues. Both studies show that a seemingly small change in the metal composition may induce a significant effect on the reactivity. Even the consequences of such small changes in the metal system are not clearly understood.

Now we report a study dealing with FeRu complexes which contain the monoazadienyl ligand system. This study is based on the chemistry of the monoazadiene ligand<sup>3</sup> with  $\text{Ru}_3(\text{CO})_{12}$ , which has resulted in a large range

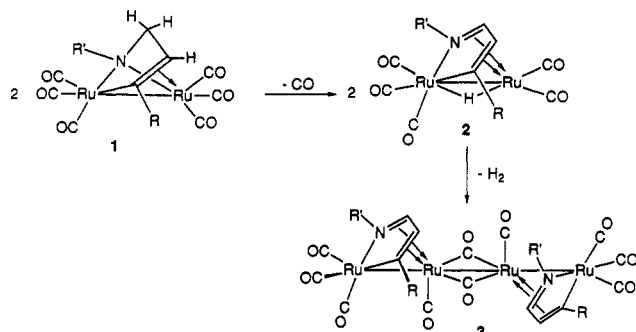
(1) Reactions of Monoazadienes with Metal Carbonyl Complexes. 13a. For earlier parts see ref 4b.

(2) (a) Gracey, B. P.; Knox, S. A. R.; Macpherson, K. A.; Orpen, A. G.; Stobart, S. R. *J. Chem. Soc., Dalton Trans.* 1985, 1935. (b) Muller, F.; van Koten, G.; Kraakman, M. J. A.; Vrieze, K.; Zoet, R.; Duineveld, K. A. A.; Heijdenrijk, D.; Stam, C. H.; Zoutberg, M. C. *Organometallics* 1989, 8, 982.

(3) MAD is used as an acronym for monoazadienes  $\text{RC}(\text{H})=\text{C}(\text{H})\text{C}(\text{H})=\text{NR}'$  in general. These ligands may be metalated at the vinyl moiety, thus forming a formal monoanionic azadienyl ligand, abbreviated as MAD-yl.



**Figure 1.** Cyclometalation of MAD on a Ru-carbonyl skeleton.



**Figure 2.** Thermal conversion of compound 1 into 3.

of complexes.<sup>4</sup> A basic feature of those reactions is the tendency of MAD to be cyclometalated on a di- or trinuclear metal core to afford four- or five-membered ruthenaazadienyl cycles and metal hydrides.<sup>4b</sup> The resulting ruthenium-hydrido complexes are not stable under the reaction conditions employed and proceed to react by hydride migration back to the monoazadienyl ligand, yielding compounds  $\text{Ru}_2(\text{CO})_6\{\text{RC}=\text{C}(\text{H})\text{C}(\text{H})_2\text{NR}'\}$  (1) and  $\text{Ru}_2(\text{CO})_6\{\text{RC}(\text{H})_2\text{CC}(\text{H})\text{NR}'\}$  (Figure 1). Subsequently, rapid conversion of 1 occurs in refluxing heptane over 2–8 h, resulting in the linear tetranuclear cluster 3 (Figure 2). This conversion proceeds via the intermediacy of the dinuclear hydrido compound 2, which dimerizes by loss of  $\text{H}_2$ .

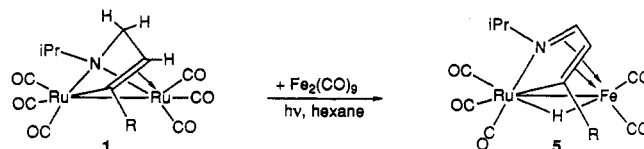
The chemistry of the  $\text{Ru}_3(\text{CO})_{12}$ /MAD system shows that the presence of the monoazadiene ligand brings about a versatile reactivity. Therefore, it seems interesting to expand the study of MAD to the FeRu frame in order to study the effect exerted by the metal core on the reactivity by comparison with the  $\text{Ru}_2$  system.

As an entry to this new class of heteronuclear monoazadienyl compounds we used the readily available  $\text{Ru}_2$  compound 1, which reacts photochemically with  $\text{Fe}_2(\text{CO})_9$  to give  $\text{HFeRu}(\text{CO})_5\{\text{RC}=\text{C}(\text{H})\text{C}(\text{H})=\text{N}-i\text{Pr}\}$  (5; see Figure 3).<sup>5</sup>

This paper deals with the reaction mechanism involved in the formation of 5. Furthermore, the reactivity of 5 has been examined in reactions with CO to evaluate the nature of the hydride ligand and the bonding properties of the metallacycle  $\text{RuN}=\text{CC}=\text{C}$  coordinated toward Fe. Finally, the differences in reactivity between analogous hetero- and homonuclear complexes will be discussed.

(4) (a) Mul, W. P.; Elsevier, C. J.; Polm, L. H.; Vrieze, K.; Zoutberg, M. C.; Heijdenrijk, D.; Stam, C. H. *Organometallics* 1991, 10, 2247. (b) Elsevier, C. J.; Mul, W. P.; Vrieze, K. *Inorg. Chim. Acta* 1992, 298–300, 689. (c) Polm, L. H.; Mul, W. P.; Elsevier, C. J.; Vrieze, K.; Christophersen, M. J. N.; Stam, C. H. *Organometallics* 1988, 7, 423. (d) Mul, W. P.; Elsevier, C. J.; van Leijen, M.; Vrieze, K.; Smeets, W. J. J.; Spek, A. L. *Organometallics* 1992, 11, 1877. (e) Mul, W. P.; Elsevier, C. J.; Vrieze, K.; Smeets, W. J. J.; Spek, A. L. *Organometallics* 1992, 11, 1891.

(5) Beers, O. C. P.; Elsevier, C. J.; Mul, W. P.; Vrieze, K.; Häming, L. P.; Stam, C. H. *Inorg. Chim. Acta* 1990, 171, 129.



**Figure 3.** Photochemically induced formation of complex 5.

## Experimental Section

$^1\text{H}$  and  $^{13}\text{C}\{^1\text{H}\}$  NMR spectra were recorded on Bruker AC 100, WM 250, and AMX 300 spectrometers. The  $^{13}\text{C}$  NMR spectra were recorded using an APT pulse sequence. IR spectra were measured on Perkin-Elmer 283 and Nicolet 7199B FTIR (liquid nitrogen cooled, HgCdTe detector) spectrometers using matched NaCl solution cells of 0.5-mm pathlength. Field desorption (FD) mass spectra were obtained with a Varian MAT711 double-focusing mass spectrometer with a combined EI/FI/FD source, fitted with a 10- $\mu\text{m}$  tungsten-wire FD emitter containing carbon microneedles with an average length of 30  $\mu\text{m}$ , using emitter currents of 0–15 mA. Elemental analyses were carried out by the Elemental Analysis section of the Institute for Applied Chemistry, TNO Zeist, The Netherlands, or Dornis und Kolbe, Mikroanalytisches Laboratorium, Mülheim a.d. Ruhr, Germany. All preparations were carried out under an atmosphere of purified nitrogen. Carefully dried solvents were used. Silica gel for column chromatography (Kieselgel 60, 70–230 mesh, E. Merck, Darmstadt, Germany) was dried and activated before use. The complex  $\text{H}_2\text{Ru}_4(\text{CO})_8\{\text{RC}=\text{C}(\text{H})\text{C}(\text{H})=\text{N}-i\text{Pr}\}_2$  was prepared according to literature procedures.<sup>4d</sup> Reported FD mass data are based on the highest peak of the isotopic pattern of the molecular ion, which corresponds to  $^{102}\text{Ru}$  and  $^{56}\text{Fe}$  (calculated value in parentheses).

**Synthesis of  $\text{HRu}_2(\text{CO})_6\{\text{RC}=\text{C}(\text{H})\text{C}(\text{H})=\text{N}-i\text{Pr}\}$  (4a, R = Ph; 4b, R = Me).** To 0.2 mmol of  $\text{H}_2\text{Ru}_4(\text{CO})_8\{\text{RC}=\text{C}(\text{H})\text{C}(\text{H})=\text{N}-i\text{Pr}\}_2$  in 30 mL of hexane was added just enough THF (about 5 mL) to obtain a clear solution. This purple solution was irradiated with a high-pressure Hg lamp with a Pyrex filter under 1.4 bar of CO for 2–3 h. The end of the reaction was indicated by a change of the color to yellow-orange. After evaporation of the solvent, hexane was added and the resulting solution filtered to remove traces of impurity. Complexes 4a,b could then be isolated in pure form in 95% yield. IR data ( $\text{cm}^{-1}$ , hexane): 4a, 2091 (m), 2050 (vs), 2021 (s), 1992 (s), 1970 (s) (lit.<sup>4d</sup> 2093 (m), 2054 (s), 2024 (m), 2019 (m), 1996 (m), 1974 (m)); 4b, 2088 (m), 2047 (vs), 2019 (vs), 1988 (s), 1969 (s).  $^1\text{H}$  NMR data ( $\text{C}_6\text{D}_6$ , ppm ( $J$ , Hz)): 4a, 7.73–6.95 (m,  $\text{C}_6\text{H}_5 + \text{CH}=\text{N}$ ), 2.70 (d, 2.0,  $\text{C}=\text{CH}$ ), 2.58 (sept, 6.5,  $\text{NCH}(\text{CH}_3)_2$ ), 0.60 (d, 6.5,  $\text{NCH}(\text{CH}_3)_2$ ), –13.00 (s, hydr); 4b, 6.90 (d, 2.1,  $\text{CH}=\text{N}$ ), 2.45 (d, 2.1,  $\text{C}=\text{CH}$ ), 3.20 (s,  $\text{CH}_3-\text{C}=\text{C}$ ), 2.54 (sept, 6.3,  $\text{NCH}(\text{CH}_3)_2$ ), 0.55 (d, 6.3,  $\text{NCH}(\text{CH}_3)_2$ ), –12.99 (s, hydr).

**Synthesis of  $\text{HFeRu}(\text{CO})_5\{\text{RC}=\text{C}(\text{H})\text{C}(\text{H})=\text{N}-i\text{Pr}\}$  (5a, R = Ph; 5b, R = Me).** I. As reported before,<sup>5</sup> complex 5 can be prepared in 35% yield by irradiating a solution of complex 1 with a large excess of suspended  $\text{Fe}_2(\text{CO})_9$ . The yield of 5 can be raised to ca. 60% by reacting the dark brown-red byproduct, which could not be further purified by column chromatography,<sup>5</sup> with  $\text{H}_2$  at 100 °C in heptane. This reaction was stopped after 0.5 h, when the dark color of the starting product had disappeared. Purification of the reaction products by column chromatography on silica yielded substantial amounts of  $\text{H}_2\text{Ru}_4(\text{CO})_{12}$  in the hexane fraction.<sup>6</sup> The second column fraction, eluted with hexane/ $\text{CH}_2\text{Cl}_2$  (7:1), contained pure  $\text{HFeRu}(\text{CO})_5\{\text{RC}=\text{C}(\text{H})\text{C}(\text{H})=\text{N}-i\text{Pr}\}$  (5a,b).

II. A solution of 0.2 mmol of 4a,b in 20 mL of hexane was stirred with a large excess of suspended  $\text{Fe}_2(\text{CO})_9$  ( $\pm 10$  equiv) in the dark for 16 h. After filtration the resulting solution was chromatographed on silica. Elution with hexane/ $\text{CH}_2\text{Cl}_2$  ((10–5):1) yielded complexes 5a,b in 70–80% yield.

(6) Knox, S. A. R.; Koepke, J. W.; Andrews, M. A.; Kaesz, H. D. *J. Am. Chem. Soc.* 1975, 97, 3942.

**Reaction of  $\text{HFeRu}(\text{CO})_5\{\text{PhC}=\text{C}(\text{H})\text{C}(\text{H})=\text{N}-i\text{Pr}\}$  (5a) with CO: Synthesis of  $\text{FeRu}(\text{CO})_6\{\text{PhC}(\text{H})\text{C}(\text{H})\text{C}(\text{H})\text{N}-i\text{Pr}\}$  (6a).**  $T = 85^\circ\text{C}$ . A solution of 0.24 g of 5a (0.5 mmol) in 30 mL of heptane was stirred under 1.2 bar of CO at  $85^\circ\text{C}$  for 2.5 h. The reaction mixture was then transferred to a silica column. Elution with hexane yielded a yellow fraction containing 0.08 g of  $\text{Ru}_3(\text{CO})_{12}$  (corresponding to 25% of converted 5a). With the eluent hexane/ $\text{CH}_2\text{Cl}_2$  (5:1) an orange fraction was obtained, containing 0.17 g of complex 6a (70% yield). Orange crystals, suitable for X-ray determination, were grown from a concentrated hexane solution at  $-80^\circ\text{C}$ .

$T = 100^\circ\text{C}$ . The same procedure as above was employed. No  $\text{Ru}_3(\text{CO})_{12}$  could be detected in this case. The yield of complex 6a was 90%. Anal. Found (calcd) for  $\text{C}_{18}\text{H}_{15}\text{NO}_6\text{FeRu}$  (6a): C, 43.36 (43.39); H, 3.04 (3.01); N, 2.84 (2.81). FD-mass:  $m/e$  499 ( $M_r = 499$ ).

**Reaction of  $\text{HFeRu}(\text{CO})_5\{\text{MeC}=\text{C}(\text{H})\text{C}(\text{H})=\text{N}-i\text{Pr}\}$  (5b) with CO: Synthesis of  $\text{FeRu}(\text{CO})_6\{\text{MeC}(\text{H})\text{C}(\text{H})\text{C}(\text{H})\text{N}-i\text{Pr}\}$  (6b) and  $\text{FeRu}(\text{CO})_6\{\text{MeC}=\text{C}(\text{H})\text{CH}_2\text{N}-i\text{Pr}\}$  (7).** A solution of 0.20 g of 5b (0.5 mmol) in 30 mL of heptane was stirred under 1.2 bar of CO at  $100^\circ\text{C}$ . After 3 h the reaction was stopped and the reaction products were separated by column chromatography on silica. With hexane as the eluent, complex 1 (50%) and 7 (25%) were obtained as yellow oils (together 0.12 g; mutual ratio determined by  $^1\text{H}$  NMR). Minor amounts of  $\text{Ru}_3(\text{CO})_{12}$  (<5%) were detected by IR spectroscopy. Subsequent elution with hexane/ $\text{CH}_2\text{Cl}_2$  (10:1) afforded the orange-brown complex 6b (40 mg, 20%). With hexane/ $\text{CH}_2\text{Cl}_2$  (9:1) a tiny amount of  $\text{Ru}_2(\text{CO})_6(\text{EtCC}(\text{H})\text{N}-i\text{Pr})$  (Figure 1) was obtained (<5%). FD mass for  $\text{C}_{13}\text{H}_{13}\text{NO}_6\text{FeRu}$  (7):  $m/e$  437 ( $M_r = 437$ ).

**In Situ Preparation of  $\text{FeRu}(\text{CO})_6\{\text{RC}=\text{C}(\text{H})\text{C}(\text{H})=\text{N}-i\text{Pr}\}^+\text{BF}_4^-$  (8a,b).** A solution of 1.0 mmol of  $\text{HFeRu}(\text{CO})_5(\text{RC}=\text{CHCH}=\text{N}-i\text{Pr})$  (5a,b) in 20 mL of  $\text{CH}_2\text{Cl}_2$  was treated with 1.1 equiv of  $\text{Ph}_3\text{C}^+\text{BF}_4^-$  in 10 mL of  $\text{CH}_2\text{Cl}_2$  under an atmosphere of CO. The reaction was complete within 5 min, indicated by the IR spectrum of the cationic species. For complex 8a absorption bands at 2125 (m), 2090 (vs), 2068 (m), and 2040 (s)  $\text{cm}^{-1}$  were observed, whereas the CO stretching frequencies for 8b were found at 2131 (m), 2110 (w), 2089 (vs), 2063 (s), and 2040 (vs)  $\text{cm}^{-1}$ . The reaction mixture was evaporated to dryness, and the residue was washed twice with 20 mL of hexane/ $\text{CH}_2\text{Cl}_2$  (5:1) in order to remove  $\text{Ph}_3\text{C}^+\text{H}$ . The complexes 8a,b, obtained in about 70% yield, were then dissolved in  $\text{CH}_2\text{Cl}_2$ .

**Formation of  $\text{HFeRu}(\text{CO})_6\{\text{PhC}=\text{C}(\text{H})\text{C}(\text{H})=\text{N}-i\text{Pr}\}$  (9a).** A dichloromethane solution of 0.18 g of 8a (0.3 mmol), obtained as described above, was transferred to a silica column. Elution with  $\text{CH}_2\text{Cl}_2$  did not yield any complexes. Upon subsequent elution with  $\text{CH}_2\text{Cl}_2/\text{THF}$  (9:1) the product, complex 9a, was formed on the column and eluted. After evaporation of the solvent complex 9a could be further purified either by another chromatographic procedure (eluent hexane/ $\text{CH}_2\text{Cl}_2$  in the ratio 9:1) or by extraction with three portions of 5 mL of cold hexane. The orange-red complex 9a was obtained in about 30–40% yield (0.06 g). Red crystals suitable for an X-ray structure determination were grown from a concentrated methanol solution at  $-80^\circ\text{C}$ . Anal. Found (calcd) for  $\text{C}_{18}\text{H}_{15}\text{NO}_6\text{FeRu}$  (9a): C, 43.58 (43.39); H, 3.10 (3.01); N, 2.92 (2.81); FD mass:  $m/e$  499 ( $M_r = 499$ ).

**Synthesis of  $\text{FeRu}(\text{CO})_6\{\text{PhCC}(\text{H})\text{C}(\text{H})\text{N}(\text{H})-i\text{Pr}\}$  (10aI).** To a solution of 0.18 g of 8a (0.3 mmol) in 20 mL of  $\text{CH}_2\text{Cl}_2$  was added 0.13 g of  $\text{NaBH}_4$  (1.2 mmol) at  $-80^\circ\text{C}$ . After it was stirred for 3 h at  $-80^\circ\text{C}$ , the suspension was gradually warmed to room temperature and filtered. The filtrate was evaporated to dryness and the residue purified by column chromatography on silica. Elution with hexane/ $\text{CH}_2\text{Cl}_2$  (5:1) afforded 0.10 g of the yellow complex 10aI (70%). Anal. Found (calcd) for  $\text{C}_{18}\text{H}_{15}\text{NO}_6\text{FeRu}$  (10aI): C, 43.32 (43.39); H, 3.03 (3.01); N, 2.87 (2.81). FD mass:  $m/e$  499 ( $M_r = 499$ ).

**Thermal Stability of 6b and 7 under CO.** A solution of 0.1 mmol of 6b or a mixture of 7 and 1 (obtained as described above) in 10 mL of heptane was stirred under 1.5 bar of CO at  $100^\circ\text{C}$  for 6 h.  $^1\text{H}$  NMR spectroscopy of the reaction mixture of 7 and 1 indicated that the composition had not changed. The  $^1\text{H}$  NMR

spectrum of the reaction mixture for the reaction with 6b revealed the presence of 6b (60%), 1 (25%), and 7 (15%).

**Conversion of 9a into 6a.** A solution of 50 mg of 9a (0.1 mmol) in 15 mL of heptane was stirred under 1.5 bar of CO at  $70^\circ\text{C}$  for 1.5 h. Spectroscopic analysis of the reaction mixture ( $^1\text{H}$  NMR and IR) indicated quantitative conversion into complex 6a.

**Conversion of 9a into 5a. I.** A solution of 50 mg of 9a (0.1 mmol) in 15 mL of heptane was stirred at  $70^\circ\text{C}$  for 1.5 h. During this time complex 9a was quantitatively converted into complex 5a, as monitored by IR and  $^1\text{H}$  NMR.

**II.** Upon irradiation of a Pyrex-filtered solution of 50 mg of 9a (0.1 mmol) in 15 mL of heptane over 10 min, quantitative conversion into complex 5a was observed (IR and  $^1\text{H}$  NMR spectroscopy).

**Thermal Conversion of 6a,b into 5a,b.** A heptane solution of 0.1 mmol of 6a,b was stirred at  $100^\circ\text{C}$  for 1 h. Almost quantitative conversion into 5a,b was observed by means of IR/ $^1\text{H}$  NMR spectroscopy of the reaction mixture.

**Photochemical Conversion of 6a into 5a.** A solution of 50 mg of 9a (0.1 mmol) in 15 mL of heptane was irradiated under 1.5 bar of CO in a Pyrex-filtered tube. After 3 h the reaction was stopped and according to IR and  $^1\text{H}$  NMR spectroscopy about 20% of 6a was still unconverted. Complex 5a was detected in about 70% yield, together with a minor amount of complex 9a ( $\pm 5\%$ ).

**Thermal Reaction of 10aI.** A solution of 0.1 mmol of 10aI in 15 mL of heptane was stirred at  $100^\circ\text{C}$  for 4 h. Examination of the resulting solution with IR and  $^1\text{H}$  NMR spectroscopy indicated that no reaction had taken place.

**Crystal Structure Determination of 6a and 9a.** X-ray data were collected on an Enraf-Nonius CAD4 diffractometer. Crystal data are collected in Table I. Both structures were solved with standard Patterson and Fourier techniques (SHELXS86<sup>7</sup>) and refined on  $F$  by full-matrix least-squares techniques. Neutral atom scattering factors were taken from ref 8 and corrected for anomalous dispersion.<sup>9</sup> All calculations were performed with SHELX76<sup>10</sup> and PLATON<sup>11</sup> (geometrical calculations and illustrations) on a MicroVAX-II cluster. Final atomic coordinates and equivalent isotropic thermal parameters are listed in Tables II and III and selected bond distances and angles in Tables IV and V.

**Complex 6a.** Data were collected with  $\omega$  scan mode at 100 K for a red-brown, plate-shaped crystal mounted on top of a glass fiber. Lattice parameters were determined by least-squares fitting of the SET4 setting angles of 25 reflections with  $7.5 < \theta < 14.5^\circ$ . The unit cell parameters were checked for the presence of higher lattice symmetry.<sup>12</sup> Data were corrected for  $L_p$ ; no significant decay (<1%) of the intensity control reflections was observed during the 151 h of X-ray exposure time. Absorption correction was applied using ABSORB (Gaussian integration). Standard deviations of the intensities as obtained by counting statistics were increased according to an analysis of the excess variance of the reference reflections:  $\sigma^2(I) = \sigma_{\text{ca}}^2(I) + (0.014I)^2$ .<sup>13</sup> H atoms were included in the refinement on calculated positions (C–H = 0.98 Å) riding on their carrier atoms with one common isotropic thermal parameter. All non-hydrogen atoms were refined with anisotropic thermal parameters. Weights were introduced in the final refinement cycles.

**Complex 9a.** Data were collected for a red plate-shaped crystal mounted on top of a glass fiber. Unit cell parameters were determined from a least-squares treatment of the SET4 setting

(7) Sheldrick, G. M. SHELXS86: Program for Crystal Structure Determination; University of Göttingen, Göttingen, Federal Republic of Germany, 1986.

(8) Cromer, D. T.; Mann, J. B. *Acta Crystallogr.* 1968, A24, 321.

(9) Cromer, D. T.; Liberman, D. *J. Chem. Phys.* 1970, 53, 1891.

(10) Sheldrick, G. M. SHELX76: Crystal Structure Analysis Package; University of Cambridge, Cambridge, England, 1976.

(11) Spek, A. L. *Acta Crystallogr.* 1990, A46, C34.

(12) Spek, A. L. *J. Appl. Crystallogr.* 1988, 21, 578.

(13) McCandlish, L. E.; Stout, G. H.; Andrews, L. C. *Acta Crystallogr.* 1975, A31, 245.

**Table I. Crystal Data and Details of the Structure Determinations of 6a and 9a**

	6a	9a
Crystal Data		
formula	C <sub>18</sub> H <sub>15</sub> NO <sub>6</sub> FeRu	C <sub>18</sub> H <sub>15</sub> NO <sub>6</sub> FeRu
mol wt	498.24	498.24
cryst syst	monoclinic	orthorhombic
space group	P2 <sub>1</sub> /c (No. 14)	P2 <sub>1</sub> 2 <sub>1</sub> 2 <sub>1</sub> (no. 19)
a, Å	12.106(14)	9.819(1)
b, Å	9.490(10)	11.928(1)
c, Å	16.780(7)	17.338(1)
β, deg	97.61(7)	90
V, Å <sup>3</sup>	1911(3)	2030.7(3)
D <sub>calc</sub>	1.732	1.630
Z	4	4
F(000)	992	992
μ, cm <sup>-1</sup>	15.7	14.7
cryst size, mm	0.06 × 0.42 × 0.74	0.80 × 0.21 × 0.08
Data Collection		
temp, K	100	295
radiation	Mo Kα (Zr), 0.710 73 Å	Mo Kα (Zr), 0.710 73 Å
θ <sub>min</sub> /θ <sub>max</sub> , deg	1.2, 27.5	1.17, 27.49
scan type	ω	ω/2θ
Δω, deg	4.0 + 0.35 tan θ	0.60 + 0.35 tan θ
horiz and vert aperture, mm	3.0 + 0.35 tan θ (limits 1.3, 5.9), 5.00	3.00, 6.00
ref rflns	2,2,-6; 220; 402	301; 021; 320
data set	0-15; -12 to 0; -21 to 21	0-12; 0-15; 0-22
total no. of data	5098	2820
no. of unique data	4351 (R <sub>int</sub> = 0.078)	2640
no. obsd data	2215 (I > 3σ(I))	1434 (I > 2.5σ(I))
Refinement		
N <sub>ref</sub> , N <sub>par</sub>	2215, 245	1434, 254
R, R <sub>w</sub> , S	0.055, 0.040, 2.55	0.0443, 0.0459, 1.51
weighting scheme	w <sup>-1</sup> = σ <sup>2</sup> (F)	w <sup>-1</sup> = σ <sup>2</sup> (F) + 0.000613F <sup>2</sup>
max and av shift/error	0.013, 0.0017	0.106, 0.018
max/min residual density, e Å <sup>-3</sup>	1.39, -1.38 (near Ru)	0.77, -0.37 (near Ru)

**Table II. Final Coordinates and Equivalent Isotropic Thermal Parameters for the Non-Hydrogen Atoms of 6a**

atom	x	y	z	U(eq), Å <sup>2</sup>
Ru	0.23187(5)	0.24438(9)	0.07816(4)	0.0319(2)
Fe	0.15680(10)	0.18669(13)	0.21325(7)	0.0337(4)
O(1)	0.1688(5)	0.5480(7)	0.0377(3)	0.044(2)
O(2)	0.0385(5)	0.1388(6)	-0.0446(3)	0.054(3)
O(3)	0.3948(5)	0.2043(7)	-0.0436(3)	0.057(3)
O(4)	0.0974(6)	0.0680(7)	0.3626(3)	0.064(3)
O(5)	-0.0644(5)	0.1458(7)	0.1231(4)	0.059(3)
O(6)	0.1305(6)	0.4886(7)	0.2405(5)	0.079(3)
N(1)	0.2486(5)	0.0639(8)	0.1498(3)	0.033(3)
C(1)	0.5161(7)	0.4229(10)	0.1120(5)	0.050(4)
C(2)	0.6189(7)	0.4162(11)	0.0845(5)	0.048(4)
C(3)	0.6828(7)	0.2954(11)	0.0984(5)	0.054(4)
C(4)	0.6418(7)	0.1826(12)	0.1361(5)	0.050(4)
C(5)	0.5382(7)	0.1907(11)	0.1638(5)	0.048(4)
C(6)	0.4733(7)	0.3106(11)	0.1511(5)	0.042(3)
C(7)	0.3572(6)	0.3201(10)	0.1723(5)	0.041(3)
C(8)	0.3332(6)	0.2279(10)	0.2397(5)	0.046(4)
C(9)	0.3075(6)	0.0862(9)	0.2232(4)	0.032(3)
C(10)	0.2295(7)	-0.0864(9)	0.1222(5)	0.039(3)
C(11)	0.1760(7)	-0.1771(8)	0.1818(4)	0.042(3)
C(12)	0.3406(7)	-0.1456(10)	0.1058(5)	0.053(4)
C(13)	0.1925(7)	0.4322(10)	0.0506(5)	0.040(3)
C(14)	0.1080(7)	0.1709(10)	0.0041(5)	0.039(3)
C(15)	0.3349(7)	0.2188(8)	0.0029(5)	0.039(3)
C(16)	0.1224(7)	0.1134(10)	0.3049(5)	0.044(3)
C(17)	0.0212(7)	0.1593(9)	0.1600(5)	0.036(3)
C(18)	0.1382(8)	0.3697(11)	0.2298(6)	0.052(4)

<sup>a</sup> U(eq) = one-third of the trace of the orthogonalized U tensor.

angles of 25 reflections in the range 10.6 < θ < 14.5° and were checked for the presence of higher lattice symmetry.<sup>12</sup> Data were corrected for Lp and for a linear decay (6%) of the intensity

**Table III. Final Coordinates and Equivalent Isotropic Thermal Parameters of the Non-Hydrogen Atoms of 9a**

atom	x	y	z	U(eq), Å <sup>2</sup>
Fe	-0.44480(16)	0.85168(14)	0.15745(10)	0.0644(6)
Ru	-0.17406(9)	0.91544(8)	0.16816(5)	0.0559(3)
O(1)	0.1041(10)	0.8227(9)	0.1241(5)	0.092(4)
O(2)	-0.1600(9)	0.8153(9)	0.3275(5)	0.102(4)
O(3)	-0.0965(11)	1.1460(8)	0.2385(6)	0.106(4)
O(4)	-0.6195(11)	0.6577(10)	0.1367(7)	0.127(6)
O(5)	-0.6256(12)	1.0355(10)	0.1094(6)	0.120(5)
O(6)	-0.4913(10)	0.8346(12)	0.3236(7)	0.132(5)
N(1)	-0.2033(10)	0.9702(9)	0.0521(6)	0.066(4)
C(1)	-0.0093(18)	1.0841(17)	0.0185(10)	0.131(8)
C(2)	-0.236(2)	1.1728(13)	0.0333(11)	0.145(9)
C(3)	-0.1564(16)	1.0701(11)	0.0101(9)	0.097(6)
C(4)	-0.2925(12)	0.9086(11)	0.0185(6)	0.067(4)
C(5)	-0.3413(11)	0.8095(9)	0.0552(6)	0.063(4)
C(6)	-0.2757(11)	0.7730(10)	0.1262(6)	0.055(4)
C(7)	-0.2365(10)	0.6557(9)	0.1362(6)	0.053(4)
C(8)	-0.2572(12)	0.5992(10)	0.2053(7)	0.065(5)
C(9)	-0.2174(12)	0.4902(12)	0.2130(9)	0.078(6)
C(10)	-0.1557(13)	0.4355(10)	0.1568(10)	0.084(6)
C(11)	-0.1333(13)	0.4872(12)	0.0864(9)	0.086(6)
C(12)	-0.1746(13)	0.5976(10)	0.0786(7)	0.073(4)
C(13)	0.0046(14)	0.8592(10)	0.1421(7)	0.064(4)
C(14)	-0.1644(11)	0.8554(12)	0.2672(8)	0.070(5)
C(15)	-0.1209(13)	1.0647(11)	0.2100(8)	0.077(5)
C(16)	-0.5539(14)	0.7375(13)	0.1447(8)	0.085(6)
C(17)	-0.5552(14)	0.9638(13)	0.1274(8)	0.084(6)
C(18)	-0.4714(12)	0.8410(15)	0.2579(10)	0.088(6)

<sup>a</sup> U(eq) = one-third of the trace of the orthogonalized U tensor.

control reflections during the 43 h of X-ray exposure time, but not for absorption. The hydride H atom was localized from a difference Fourier map. Other H atoms were introduced on calculated positions (C-H = 0.98 Å) and included in the refinement riding on their carrier atoms with one common isotropic thermal parameter (U = 0.106(12) Å<sup>2</sup>). All non-H atoms were refined with anisotropic thermal parameters. Weights were introduced in the final refinement cycles; convergence was reached at R = 0.0443, R<sub>w</sub> = 0.0459, w<sup>-1</sup> = σ<sup>2</sup>(F) + 0.000613F<sup>2</sup>. The absolute structure was checked by refinement with opposite anomalous dispersion factors (f''), resulting in R = 0.0466 and R<sub>w</sub> = 0.0473.

## Results

**Formation of the Complexes 5-10.** First, the formation reactions of the new heterodinuclear complexes will be discussed briefly and the details about the characterization of these compounds will follow afterwards.

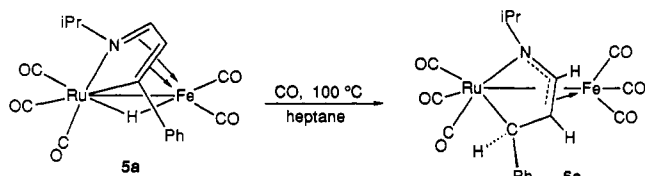
**Formation of 5.** Upon irradiation of a hexane solution of Ru<sub>2</sub>(CO)<sub>8</sub>RC=CHCH<sub>2</sub>N-iPr (1) in the presence of excess suspended Fe<sub>2</sub>(CO)<sub>9</sub>, the new heteronuclear complex HFeRu(CO)<sub>5</sub>RC=C(H)C(H)=N-iPr (5; see Figure 3) was formed in good yield together with Fe<sub>2</sub>Ru(CO)<sub>12</sub> and FeRu<sub>3</sub>(CO)<sub>10</sub>RC=C(H)C(H)=N-iPr.<sup>5</sup> Complex 5 has been characterized both by spectroscopy and by an X-ray structure determination.<sup>5</sup> In order to explain the presence of the FeRu<sub>3</sub> complex, the intermediacy of a Ru<sub>2</sub>-hydrido complex must be assumed. The heterotetranuclear complex may then be formed by dimerization of a HFeRu and a HRu<sub>2</sub> fragment with loss of H<sub>2</sub>, by analogy with the conversion of 2 into 3 (Figure 2). Recently, we have developed an alternative route for the preparation of HRu<sub>2</sub>(CO)<sub>8</sub>RC=C(H)C(H)=N-iPr (4) in high yield, by the irradiation of the butterfly complex H<sub>2</sub>Ru<sub>4</sub>(CO)<sub>8</sub>RC=C(H)C(H)=N-iPr<sub>2</sub><sup>4d</sup> under an atmosphere of CO, which enabled us to verify whether 5 could also be formed by the reaction of 4 with Fe<sub>2</sub>(CO)<sub>9</sub>. Upon reaction of 4 with Fe<sub>2</sub>(CO)<sub>9</sub> in the dark, complex 5 was obtained in high yields, as was anticipated.

Table IV. Selected Bond Distances (Å) and Bond Angles (deg) for **6a** (with Esd's in Parentheses)

Ru-Fe	2.610(3)	Ru-N(1)	2.087(7)	Ru-C(7)	2.163(9)
Ru-C(13)	1.887(10)	Ru-C(14)	1.946(9)	Ru-C(15)	1.904(9)
Fe-N(1)	2.010(7)	Fe-C(8)	2.159(8)	Fe-C(9)	2.046(8)
Fe-C(16)	1.787(9)	Fe-C(17)	1.781(9)	Fe-C(18)	1.778(11)
O(1)-C(13)	1.149(12)	O(2)-C(14)	1.134(10)	O(3)-C(15)	1.142(10)
O(4)-C(16)	1.137(10)	O(5)-C(17)	1.142(11)	O(6)-C(18)	1.148(12)
N(1)-C(9)	1.356(9)	N(1)-C(10)	1.508(11)	C(6)-C(7)	1.498(11)
C(7)-C(8)	1.489(12)	C(8)-C(9)	1.400(13)		
N(1)-Ru-C(7)	81.2(3)	Ru-Fe-N(1)	51.7(2)	Ru-Fe-C(8)	72.0(2)
Ru-Fe-C(9)	76.1(2)	N(1)-Fe-C(8)	67.2(3)	N(1)-Fe-C(9)	39.0(3)
C(8)-Fe-C(9)	38.8(3)	Ru-N(1)-Fe	79.1(3)	Ru-N(1)-C(9)	113.2(6)
Ru-N(1)-C(10)	126.9(4)	Fe-N(1)-C(9)	71.9(4)	Fe-N(1)-C(10)	129.6(5)
C(9)-N(1)-C(10)	117.9(7)	Ru-C(7)-C(6)	113.3(6)	Ru-C(7)-C(8)	99.8(5)
C(6)-C(7)-C(8)	115.4(7)	Fe-C(8)-C(7)	103.7(5)	Fe-C(8)-C(9)	66.3(4)
C(7)-C(8)-C(9)	118.4(7)	Fe-C(9)-N(1)	69.1(4)	Fe-C(9)-C(8)	75.0(5)
N(1)-C(9)-C(8)	114.0(7)	N(1)-C(10)-C(11)	113.1(6)	N(1)-C(10)-C(12)	107.6(7)

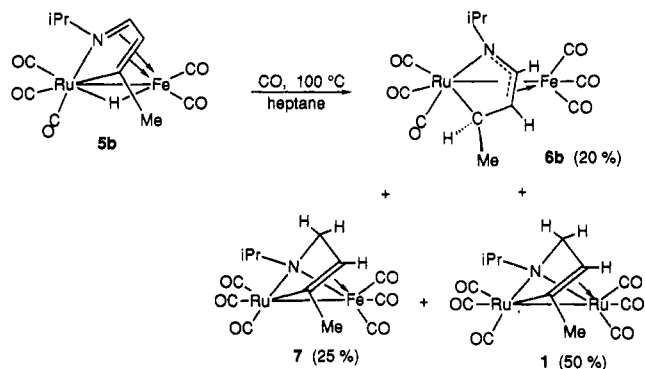
Table V. Selected Bond Distances (Å) and Bond Angles (deg) for **9a** (with Esd's in Parentheses)

Ru-Fe	2.7714(18)	Ru-N(1)	2.135(10)	Ru-C(6)	2.100(12)
Ru-C(13)	1.932(13)	Ru-C(14)	1.861(14)	Ru-C(15)	1.992(13)
Fe-C(5)	2.105(11)	Fe-C(6)	1.983(11)	Fe-C(16)	1.747(15)
Fe-C(17)	1.799(15)	Fe-C(18)	1.766(17)	O(1)-C(13)	1.114(17)
O(2)-C(14)	1.152(17)	O(3)-C(15)	1.114(16)	O(4)-C(16)	1.158(19)
O(5)-C(17)	1.143(19)	O(6)-C(18)	1.16(2)	N(1)-C(3)	1.470(18)
N(1)-C(4)	1.283(16)	C(4)-C(5)	1.425(16)	C(5)-C(6)	1.456(15)
C(6)-C(7)	1.461(16)	Ru-H(1)	1.92(3)	Fe-H(1)	1.90(4)
N(1)-Ru-C(6)	81.8(4)	C(5)-Fe-C(6)	41.6(4)	Ru-N(1)-C(3)	132.3(9)
Ru-N(1)-C(4)	110.2(8)	C(3)-N(1)-C(4)	116.9(11)	N(1)-C(4)-C(5)	120.1(10)
Fe-C(5)-C(4)	109.9(8)	Fe-C(5)-C(6)	64.7(6)	C(4)-C(5)-C(6)	118.5(10)
Ru-C(6)-Fe	85.4(4)	Ru-C(6)-C(5)	105.1(8)	Ru-C(6)-C(7)	127.5(8)
Fe-C(6)-C(5)	73.7(6)	Fe-C(6)-C(7)	129.9(8)	C(5)-C(6)-C(7)	120.2(10)
N(1)-Ru-H(1)	81(3)	C(6)-Ru-H(1)	88.2(15)	C(13)-Ru-H(1)	171(3)
C(14)-Ru-H(1)	97(3)	C(15)-Ru-H(1)	78.6(15)	C(5)-Fe-H(1)	98(3)
C(6)-Fe-H(1)	92.1(11)	C(16)-Fe-H(1)	171.3(17)	C(17)-Fe-H(1)	74.6(14)
C(18)-Fe-H(1)	86(3)				

Figure 4. Formation of  $(R_C C_{Ru} A_{Fe} / S_C A_{Ru} C_{Fe})$ -**6a** in the reaction of **5a** with CO.

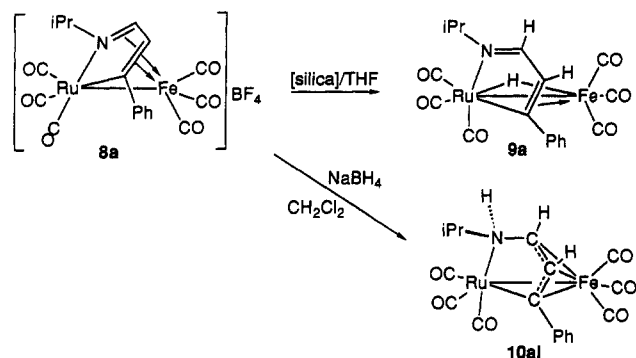
**Formation of 6 and 7.** The reactivity of **5** toward CO appeared to be remarkably dependent on the specific R substituent. In the case of **5a** (R = Ph) no reaction took place with CO at room temperature, whereas **5b** (R = Me) was completely converted into  $Fe(CO)_5$ ,  $Ru(CO)_5$ , and  $MeCH=CHCH=N-iPr$  in 24 h. Therefore, in the latter complex the hydride is returned to the metalated carbon atom  $C_\beta$  of the monoazadienyl ligand, simultaneously reducing the metal, which is in effect a reductive elimination. When **5a** was stirred under a CO atmosphere at 85 °C, reductive elimination was also observed but only to an extent of 25%. The major part (70%) underwent a hydride transfer to the  $C_\beta$  atom of the monoazadienyl ligand as well, but now the ligand was reduced instead of the metal (Figure 4). This ligand reduction reaction resulted in the novel complex **6**, featuring an unprecedented coordination mode of the monoazadienyl ligand. The structure of **6a** has been determined by X-ray crystallography (*vide infra*) and represents an aza-allylic ligand part together with an  $sp^3$ -hybridized metalated carbon atom. The yield of **6a** can be increased to 90% by raising the reaction temperature to 100 °C.

In the case of **5b** a slightly different reaction toward CO occurred at 100 °C over 3 h (Figure 5). About 50% of the  $Ru_2$  complex **1** (based on converted **5b**) and less than 5%

Figure 5. Formation of **6b**, **7**, and **1** in the thermal reaction of **5b** with CO.

of  $Ru_2(CO)_6\{EtCC(H)N-iPr\}$  (Figure 1) has been observed as the reaction products together with 20% of **6b** and 25% of the novel complex **7**, which is isostructural with **1**. Unfortunately, **7** and **1** could not be separated by column chromatography on silica, which is probably due to their structural resemblance. Therefore, **7** could only be identified by the spectroscopic analysis of a mixture of **1** and **7**.

**Reactivity of 6 and 7.** The new complexes **6a,b** and **7** were investigated with respect to their reactivity. Under the reaction conditions of the formation of **6b** and **7** (i.e. 100 °C, 1.5 bar of CO), complex **6b** appeared to be unstable. After 6 h of reaction time 25% of **6b** had been converted into **1** and 15% into **7**; the latter complexes were found to be stable under the employed reaction conditions, as was checked in a separate experiment. In a thermal reaction (100 °C, but now under an inert atmosphere over 1 h) quantitative conversion of **6a,b** into **5a,b** was observed.



**Figure 6.** Formation of the new complexes **9a** and **10aI** from compound **8a**.

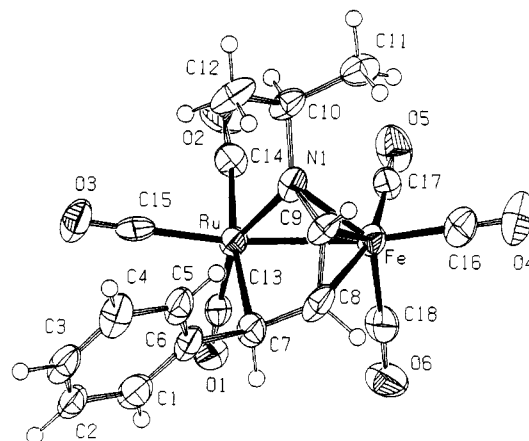
The same conversion involving **5a** took place under photochemical conditions (3 h, Hg lamp) even under 1.2 bar of CO atmosphere. Small amounts of the new complex  $\text{HFerRu}(\text{CO})_6(\text{PhC}=\text{CHCH}=\text{N}-i\text{Pr})$  (**9a**) were observed in the IR spectrum of the resulting reaction mixture. The intermediacy of **9** was indicated by the NMR spectrum of a sample of **5b** under elevated CO pressure as well.<sup>5</sup> In order to check if **9** is indeed an intermediate in the conversion of **5** into **6**, we have sought methods to synthesize complex **9**.

**Formation of 9 and 10.** First, hydride abstraction from **5a** under a CO atmosphere followed by hydride donation was attempted. By treatment of **5a,b** under a CO atmosphere with 1 equiv of the hydride abstractor  $\text{Ph}_3\text{C}^+\text{BF}_4^-$ <sup>14</sup> the cationic hexacarbonyl complexes  $\text{FeRu}(\text{CO})_6(\text{RC}=\text{CHCH}=\text{N}-i\text{Pr})^+\text{BF}_4^-$  (**8a,b**; Figure 6) were obtained in situ. The complexes **8a,b** were characterized by the IR spectrum, featuring one or two CO stretching vibration bands above  $2100\text{ cm}^{-1}$ , which is plausible for cationic complexes of this type. Addition of  $\text{NaBH}_4$  to a solution of **8a** in  $\text{CH}_2\text{Cl}_2$  did not yield **9a** but instead complex **10aI**<sup>15</sup> was obtained (Figure 6). Only one diastereomer of complex **10a** was formed, as indicated by its NMR spectra (*vide infra*).

Attempts to purify the cationic **8a** by column chromatography on silica did not afford any product when hexane/dichloromethane mixtures and pure dichloromethane were used as the eluent. Upon addition of 5% THF to the dichloromethane eluent a red band started to move. This fraction contained the desired hexacarbonyl hydrido complex **9a**. When **9a** was eluted too slowly, conversion into **10aI** took place, which is in accordance with the properties of the  $\text{Ru}_2$  analogue **4** on silica.<sup>4d</sup>

Subsequently, complex **9a** was reacted under CO atmosphere at  $70\text{ }^\circ\text{C}$  for 1.5 h, which resulted in the quantitative formation of **6a**, under conditions even milder than in the reaction of **5a** with CO. The molecular structure of **9a** has been determined by X-ray crystallography (*vide infra*).

**Molecular Structure of Complex 6a.** The molecular geometry of **6a** is given in Figure 7, and selected bond lengths and bond angles are listed in Table IV. The



**Figure 7.** Molecular structure of  $\text{FeRu}(\text{CO})_6(\text{PhC}(\text{H})\text{C}(\text{H})\text{C}(\text{H})\text{N}-i\text{Pr})$  (**6a**).

structure of **6a** consists of a  $\text{Fe}(\text{CO})_3$  unit and a  $\text{Ru}(\text{CO})_3$  fragment, forming together a "sawhorse" type of metal backbone with an intermetallic distance of  $2.610(3)\text{ \AA}$ , which is comparable to, for example, the formal single metal-metal bond of  $2.626(1)\text{ \AA}$  in  $\text{FeRu}(\text{CO})_2(\mu\text{-CO})_2(\eta^5\text{-C}_5\text{H}_5)_2$ .<sup>1</sup>

The ligand system in **6a** can be considered as a metalated  $\text{sp}^3$  carbon atom linked to an azaallyl moiety. The  $\text{N}-\text{C}(9)$  and  $\text{C}(8)-\text{C}(9)$  distances of  $1.356(9)$  and  $1.400(13)\text{ \AA}$ , respectively, are in the range observed for previously reported  $\eta^3$ -azaallyl metal carbonyl complexes.<sup>17,18</sup> For example, in  $\text{FeMn}(\text{CO})_6\{\text{tBu}-\text{NC}(\text{H})\text{C}(\text{H})-\text{N}(\text{H})-\text{tBu}\}$  the corresponding values are  $1.384(25)$  and  $1.400(17)\text{ \AA}$ , respectively.<sup>17b</sup> The distances from the azaallyl moiety to Fe in **6a** ( $\text{Fe}-\text{N} = 2.010(7)\text{ \AA}$ ;  $\text{Fe}-\text{C}(9) = 2.046(8)\text{ \AA}$ ;  $\text{Fe}-\text{C}(8) = 2.159(8)\text{ \AA}$ ) may best be compared to another Fe-bonded  $\eta^3$ -azaallyl unit, e.g. in  $\text{Fe}_2(\text{CO})_5\{\text{Me}_2\text{C}=\text{NC}(\text{H})\text{C}(\text{H})\text{N}-i\text{Pr}\}\{\eta^1\text{-MeOC}(\text{O})\text{C}=\text{C}(\text{H})\text{C}(\text{O})\text{OMe}\}$  with corresponding values of  $2.036(6)$ ,  $2.046(7)$ , and  $2.109(7)\text{ \AA}$ , respectively.<sup>17d</sup>

The most striking aspect of the structure of **6a** is the long  $\text{C}(7)-\text{C}(8)$  bond of  $1.489(2)\text{ \AA}$ , which is in agreement with the  $\text{sp}^3$  hybridization at  $\text{C}(7)$ . The  $\text{Ru}-\text{C}(7)$  bond length of  $2.163(9)\text{ \AA}$  also expresses this  $\text{sp}^3$  character at  $\text{C}(7)$ . The  $\text{Ru}-\text{C}(7)$  bond in **6a** is longer than the average value of  $2.12\text{ \AA}$  for pure  $\sigma(\text{Ru}-\text{C})$  bonds, which implies a rather weak bonding type. Normally, in complexes containing a ruthena-azadienyl cycle, such as in **3** (Figure 2), the  $\text{Ru}-\text{C}$  bond ranges from  $2.048(3)$  to  $2.072(8)\text{ \AA}$ , which is shortened to some extent as compared to pure  $\sigma\text{-Ru}-\text{C}$  bonds, which are generally found at about  $2.12\text{ \AA}$  as in  $\text{Ru}(\text{CO})_2\text{Me}(i\text{Pr-DAB})\text{OTf}$  ( $2.122(9)\text{ \AA}$ )<sup>19</sup> or  $\text{Ru}_2(\text{CO})_4\text{Me}(i\text{Pr-DAB})$  ( $2.115(5)\text{ \AA}$ )<sup>20</sup>. This shortening effect is ascribed to a carbene-like character of the  $\text{sp}^2\text{ C}_\beta$  atom.<sup>1c</sup>

**Molecular Structure of Complex 9a.** Selected bond distances and angles are given in Table V. The structure

(14) Mandon, D.; Astruc, D. *Organometallics* 1989, 8, 2372 and references cited therein.

(15) (a) It should be noted that the Fe atom is chiral as well, but since its chirality is related to the chirality of the Ru atom, this does not provide any additional information and has therefore been omitted. (b) The mechanism of the formation of **10aI** will be discussed in combination with the formation of the second diastereomer **10aII** in a forthcoming publication.<sup>16</sup>

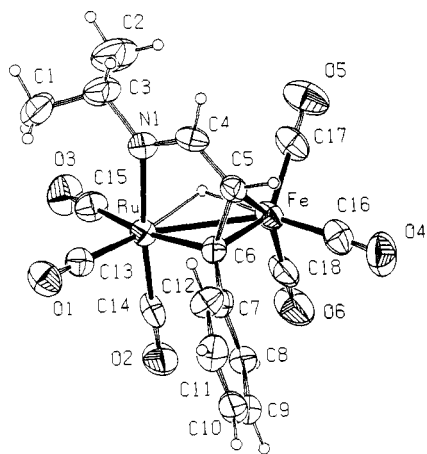
(16) Beers, O. C. P.; Elsevier, C. J.; Smeets, W. J. J.; Spek, A. L. *Organometallics*, following paper in this issue.

(17) (a) Muller, F.; van Koten, G.; Vrieze, K.; Krijnen, L. B.; Stam, C. H. *J. Chem. Soc., Chem. Commun.* 1986, 150. (b) Keijsper, J.; Mul, J.; van Koten, G.; Vrieze, K.; Ubbels, H.; Stam, C. H. *Organometallics* 1984, 3, 1732. (c) Nakamura, Y.; Backmann, K.; Heimgartner, H.; Schmid, H. *Helv. Chim. Acta* 1978, 61, 589. (d) Muller, F.; van Koten, G.; Vrieze, K.; Duineveld, K. A. A.; Heijdenrijk, D.; Mak, A. N. S.; Stam, C. H. *Organometallics* 1989, 8, 1324.

(18) Polm, L. H.; Elsevier, C. J.; Mul, W. P.; Vrieze, K.; Christophersen, M. J. N.; Muller, F.; Stam, C. H. *Polyhedron* 1988, 7, 2521.

(19) Kraakman, M. J. A.; de Klerk-Engels, B.; de Lange, P. P. M.; Smeets, W. J. J.; Spek, A. L.; Vrieze, K. *Organometallics* 1992, 11, 3774.

(20) Kraakman, M. J. A.; Vrieze, K.; Kooijman, H.; Spek, A. L. *Organometallics* 1992, 11, 3760.



**Figure 8.** Molecular structure of  $\text{HFeRu}(\text{CO})_6\{\text{PhC}=\text{C}(\text{H})\text{C}(\text{H})=\text{N}-i\text{Pr}\}$  (**9a**).

of complex **9a**, depicted in Figure 8, may be closely compared with the structure of  $\text{HRu}_2(\text{CO})_6\{\text{PhC}=\text{C}(\text{H})\text{C}(\text{Me})=\text{O}\}$ ,<sup>21</sup> which contains an  $\alpha,\beta$ -unsaturated ketone derived ligand also in the five-electron-donating coordination mode. The Fe–Ru bond in **9a** of 2.7714(18) Å is extremely long compared to, for example, the bonds in  $\text{FeRu}(\text{CO})_6\{\text{C}(\text{H})_2\text{CC}(\text{H})-\text{C}(\text{H})=\text{N}-i\text{Pr}\}$  (2.7120(8) Å)<sup>16</sup> and **6a** (2.610(3) Å). Such an elongation of the intermetallic distance has also been observed for  $\text{HRu}_2(\text{CO})_6\{\text{PhC}=\text{C}(\text{H})\text{C}(\text{Me})=\text{O}\}$  and can be ascribed to the influence of the bridging hydride in an electron-precise complex.<sup>22</sup> The bridging hydride in **9a**, which has been unambiguously located in a difference Fourier synthesis, occupies an approximately symmetrical bridging position, taking into account the shorter covalent radius of Fe compared to that of Ru. The large trans influence exerted by the bridging C(6) atom is noticeable on both the Ru–C(15) bond and the Fe–C(17) bond, which are considerably elongated as compared to the bonds of the other carbonyl ligands. The C(4)–N bond length (1.283(16) Å) is comparable to those of other localized C=N bonds in, for example,  $\text{Ru}_2(\text{CO})_6\{\text{C}(\text{H})_2\text{CC}(\text{H})\text{C}(\text{H})=\text{N}-t\text{Bu}\}$  (1.290(4) Å)<sup>18</sup> or  $\text{FeRu}(\text{CO})_6\{\text{C}(\text{H})_2\text{CC}(\text{H})\text{C}(\text{H})=\text{N}-i\text{Pr}\}$  (1.284(3) Å).<sup>16</sup> Upon coordination to Fe the C(5)–C(6) bond (1.456(15) Å) has almost been reduced to a formal single bond. The complex  $\text{HRu}_2(\text{CO})_6\{\text{PhC}=\text{C}(\text{H})\text{C}(\text{Me})=\text{O}\}$  exhibits this same feature ( $\pi(\text{C}=\text{C})$  bond of 1.462(14) Å<sup>21</sup>), which is generally explained by strong  $\pi$  back-bonding from the metal into the  $\pi^*$  orbital of the C=C unit, thus lowering the bond order. The C(6)–C(7) bond (1.461(16) Å) is only somewhat shortened compared to normal single C–C bonds, which implies poor effective overlap of the  $\pi$  systems of the phenyl and the azadienyl unit. This feature is due to the twist of 63.2(5)° between both moieties.

**Spectroscopic Analysis.** The spectroscopic data for the new heteronuclear complexes **5**–**10** are given in Tables VI–VIII. The diverse coordination behavior of the monoazadienyl ligand can be generalized by three categories (Figure 9). The compounds in the first category contain an intact Ru–N=C–C=C ring, formed by cyclometalation of the original monoazadiene. The  $\beta$ -H atom is present as a metal hydride, and the ligand system can be considered as a formally monoanionic ligand. This

situation applies to the complexes **5** and **9**. In the second group the monoazadienyl ligand is reduced by a hydride to a formally dianionic ligand (complexes **6**, **7**, and **10**). In the third category the monoazadienyl ligand from category I is dehydrogenated, yielding a formally dianionic ligand.<sup>23</sup>

**Category I.** The coordination mode of the Ru–N=C=C cycle toward Fe in category I can be easily deduced from the NMR spectra. When both the C=C and C=N  $\pi$  bonds are bonded to Fe, the resonances of  $\text{H}_{\text{im}}$  and  $\text{H}_\alpha$  are found in the range 7–6 and 6–5 ppm, respectively. In this mode the monoazadienyl ligand serves as a 7e donor to the metal skeleton. The proton chemical shifts appear to be very solvent dependent: e.g., in  $\text{CDCl}_3$  the resonances of  $\text{H}_{\text{im}}$  and  $\text{H}_\alpha$  in **5** undergo a low-frequency shift of 0.77 and 0.18 ppm, respectively, compared to the values in  $\text{C}_6\text{D}_6$ . Such an effect has also been observed for complex **3**.<sup>24</sup>

More reliable data for the elucidation of the coordination mode are <sup>13</sup>C chemical shifts. Typical values for resonances of  $\text{C}_{\text{im}}$  and  $\text{C}_\alpha$  are found at about 125–105 and 105–95 ppm, respectively. These values are about in the same ranges as found for the Ru<sub>2</sub> analogues.

Within the first category another coordination mode is found. In complex **9** the monoazadienyl ligand donates only five electrons to the metal core, leaving the  $\pi$ -C=N moiety uncoordinated. The <sup>1</sup>H and <sup>13</sup>C NMR chemical shifts of  $\text{H}_{\text{im}}/\text{C}_{\text{im}}$  in **9** are found at 7.0/162.9 ppm, which is comparable to values for other  $\sigma(\text{N})$ -coordinated imine moieties.<sup>18,25</sup> The 5e coordination mode induces a large shielding effect on the resonances of  $\text{H}_\alpha/\text{C}_\alpha$ , which are found at 2.70 and 53.8 ppm, respectively, being indicative of a large amount of  $\pi$  back-bonding to the vinyl moiety. Therefore, on the basis of the NMR data the 5e- and 7e-donating coordination modes of the ligand can be distinguished easily.<sup>4b</sup>

**Category II.** Also in category II the basic structure of complexes can be readily assigned on the basis of their NMR data. In this group, complexes are found in which the ruthenaazapentadienyl ring system (intact in category I) has been reduced by a hydride. Three different alternatives for ligand reduction have been observed. The hydride can migrate to the N atom (**10**), to  $\text{C}_{\text{im}}$  (**7**), or to  $\text{C}_\beta$  (**6**). The coordination mode in **6** is unprecedented and will be examined in more detail. The other two (**7** and **10**) will be compared with their already known homonuclear Ru<sub>2</sub> analogues.

Complex **7**, possessing the ligand in the enyl-amido coordination mode, is spectroscopically rather interesting. Its homonuclear Ru<sub>2</sub> analogue was found to be fluxional, involving interchange of the  $\sigma(\text{C})$  and  $\eta^2(\text{C}=\text{C})$  bonds.<sup>4a</sup> This so-called “windshield wiper” type of oscillation induced magnetic equivalence of the CH<sub>2</sub> protons. At low temperature the slow-exchange limit on the NMR time scale was reached, affording the expected ABX pattern for the methylene hydrogens in the NMR spectrum. In the case of complex **7**, however, this characteristic spectrum has been obtained at room temperature and it does not change upon heating to 50 °C. This means that

(23) The two complexes belonging to this class are the subject of another paper.<sup>16</sup>

(24) Mul, W. P.; Elsevier, C. J.; Ernsting, J.-M.; de Lange, W. G. J.; van Straalen, M. D. M.; Vrieze, K.; de Wit, M.; Stam, C. H. *J. Am. Chem. Soc.*, in press.

(25) See e.g.: Zoet, R.; Jastrzebski, J. T. B. H.; van Koten, G.; Mahabiersing, T.; Stam, C. H.; Vrieze, K. *Organometallics* 1988, 7, 2108.

(21) Domingos, A. J. P.; Johnson, B. F. G.; Lewis, J.; Sheldrick, G. M. *J. Chem. Soc., Chem. Commun.* 1973, 912.

(22) Bennett, M. A.; Bruce, M. I.; Matheson, T. W. In *Comprehensive Organometallic Chemistry*; Wilkinson, G., Stone, F. G. A., Abel, E. W., Eds.; Pergamon: Oxford, England, 1982; Vol. 4, p 846.

Table VI. IR Data<sup>a</sup> for 5–7, 9, and 10 (a, R = Ph; b, R = Me)

comp	$\nu(\text{CO}), \text{cm}^{-1}$					$\nu(\text{N-H})$
5a	2088 (s)	2017 (vs, br)	1993 (vs)	1936 (s)		
5b	2086 (s)	2016 (s)	2010 (s)	1989 (vs)	1932 (s)	
6a	2073 (s)	2022 (vs)	2000 (s)	1996 (s)	1966 (s)	
6b	2072 (s)	2021 (vs)	2005 (vs)	1987 (s)	1965 (s)	
7	2074 (m)	2032 (s)	1998 (s)	1984 (s)	1978 (m)	1940 (w)
9a	2092 (s)	2038 (vs)	2023 (s)	2018 (s)	1979 (s)	1961 (s)
10aI	2072 (s)	2019 (vs)	2008 (s)	1981 (m)	1965 (s)	1937 (w)
						3290 (vw) <sup>b</sup>

<sup>a</sup> In units of  $\text{cm}^{-1}$ . Conditions and definitions: hexane solution;  $\text{HFeRu}(\text{CO})_5[\text{FC}=\text{C}(\text{H})\text{C}(\text{H})=\text{N-iPr}]$  (5),  $\text{FeRu}(\text{CO})_6[\text{RC}(\text{H})\text{C}(\text{H})\text{C}(\text{H})\text{N-iPr}]$  (6),  $\text{FeRu}(\text{CO})_6[\text{MeC}=\text{C}(\text{H})\text{CH}_2\text{N-iPr}]$  (7),  $\text{HFeRu}(\text{CO})_6[\text{RC}=\text{C}(\text{H})\text{C}(\text{H})=\text{N-iPr}]$  (9),  $\text{FeRu}(\text{CO})_6[\text{RCC}(\text{H})\text{C}(\text{H})\text{N}(\text{H})\text{-iPr}]$  (10). <sup>b</sup> Could only be detected when measured in a KBr pellet.

Table VII. <sup>1</sup>H NMR Data<sup>a</sup> for 5–7, 9, and 10 (a, R = Ph; b, R = Me)

	$\text{H}_{\text{im/am}}$	$\text{H}_\alpha$	$\text{H}_\beta$	iPr	R	N-H/M-H
5a <sup>b</sup>	5.71 (d, 1.5)	5.66 (d, 1.5)		2.02 (sept, 6.5) 0.61/0.57 (d, 6.5)	7.11–6.90 (m)	–9.12 (s)
5b <sup>c</sup>	6.48 (d, 1.7)	5.84 (d, br)		2.53 (sept, 6.5) 1.10/0.99 (d, 6.5)	2.04 (s)	–9.40 (s)
6a	6.91 (d, 2.4)	3.85 (dd, 4.1, 2.4)	3.41 (d, 4.1)	3.90 (sept, 6.5) 1.65/1.64 (d, 6.5)	7.19–6.81 (m)	
6b	6.48 (d, 2.6)	3.89 (dd, 2.6, 4.5)	2.02 (dq, 4.5, 6.9)	3.84 (sept, 6.5) 1.63/1.55 (d, 6.5)	0.99 (d, 6.9)	
7	3.70 (dd, 9.3, 2.3) 3.44 (d, 9.3)	4.69 (d, 2.3)		2.53 (sept, 6.5) 1.10/0.96 (d, 6.5)	2.45 (s)	
9a <sup>d</sup>	7.01 (d, 1.2)	2.70 (d, 1.2)		2.63 (sept, 6.5) 0.81/0.78 (d, 6.6)	8.00–7.2 (m)	–15.92 (s)
10aI	4.29 (dd, 2.5, 2.5)	5.60 (d, 2.5)		2.26 (dsept, 6.5, 6.8) 1.07/0.99 (d, 6.5)	7.69–7.23 (m)	2.60 (br)

<sup>a</sup> In units of ppm (*J* values in Hz). Conditions and definitions: 300.1 MHz,  $\text{CDCl}_3$ , 293 K, unless stated otherwise  $\text{HFeRu}(\text{CO})_5[\text{RC}=\text{C}(\text{H})\text{C}(\text{H})=\text{N-iPr}]$  (5),  $\text{FeRu}(\text{CO})_6[\text{RC}(\text{H})\text{C}(\text{H})\text{C}(\text{H})\text{N-iPr}]$  (6),  $\text{FeRu}(\text{CO})_6[\text{MeC}=\text{C}(\text{H})\text{CH}_2\text{N-iPr}]$  (7),  $\text{HFeRu}(\text{CO})_6[\text{RC}=\text{C}(\text{H})\text{C}(\text{H})=\text{N-iPr}]$  (9),  $\text{FeRu}(\text{CO})_6[\text{RCC}(\text{H})\text{C}(\text{H})\text{N}(\text{H})\text{-iPr}]$  (10). <sup>b</sup> 250.1 MHz,  $\text{C}_6\text{D}_6$ . <sup>c</sup> 100.1 MHz. <sup>d</sup> 250.1 MHz, toluene-*d*<sub>8</sub>.

Table VIII. <sup>13</sup>C NMR Data<sup>a</sup> for 5–7, 9, and 10 (a, R = Ph; b, R = Me)

	$\text{C}_{\text{im/am}}$	$\text{C}_\alpha$	$\text{C}_\beta$	$\text{C}_{\text{iPr}}$	R	$\text{CO}_{\text{Fe}}$	$\text{CO}_{\text{Ru}}$
5a <sup>b</sup>	109.1	103.6	150.8	61.9, 26.7/23.5	150.5, 128.3, 128.2, 126.6	215.0, 212.9	195.0, 191.6, 190.7
5b <sup>c</sup>	109.4	105.8	149.7	62.2, 27.1/24.4	33.0	215.7, 214.9	196.7, 192.4, 190.8
6a <sup>d</sup>	110.1	71.8	37.9	64.7, 29.2/25.3	155.7, 128.8, 124.0, 123.9	212.6	201.1, 190.8, 190.1
6b <sup>e</sup>	107.2	78.0	34.2	64.1, 29.0/27.5	25.0	212.5	201.1, 192.8, 189.1
7 <sup>e</sup>	62.9	80.1	178.7	63.7, 23.7/22.7	34.4	211.4	199.6, 194.9, 194.7
9a <sup>c</sup>	181.4	53.8	162.9	61.0, 22.8/22.4	154.6, 129.2, 128.7, 125.5	213.1	194.8, 193.5, 193.4
10aI <sup>d</sup>	67.5	89.2	169.2	60.8, 21.6/21.3	149.3, 129.6, 128.9, 127.9	214.7	198.7, 197.6, 193.5

<sup>a</sup> In units of ppm. Definitions:  $\text{HFeRu}(\text{CO})_5[\text{RC}=\text{C}(\text{H})\text{C}(\text{H})=\text{N-iPr}]$  (5),  $\text{FeRu}(\text{CO})_6[\text{RC}(\text{H})\text{C}(\text{H})\text{C}(\text{H})\text{N-iPr}]$  (6),  $\text{FeRu}(\text{CO})_6[\text{MeC}=\text{C}(\text{H})\text{CH}_2\text{N-iPr}]$  (7),  $\text{HFeRu}(\text{CO})_6[\text{RC}=\text{C}(\text{H})\text{C}(\text{H})=\text{N-iPr}]$  (9),  $\text{FeRu}(\text{CO})_6[\text{RCC}(\text{H})\text{C}(\text{H})\text{N}(\text{H})\text{-iPr}]$  (10). <sup>b</sup> 62.9 MHz,  $\text{C}_6\text{D}_6$ , 293 K. <sup>c</sup> 62.9 MHz, toluene-*d*<sub>8</sub>, 263 K. <sup>d</sup> 75.46 MHz,  $\text{CDCl}_3$ , 293 K. <sup>e</sup> 75.46 MHz,  $\text{CDCl}_3$ , 263 K.

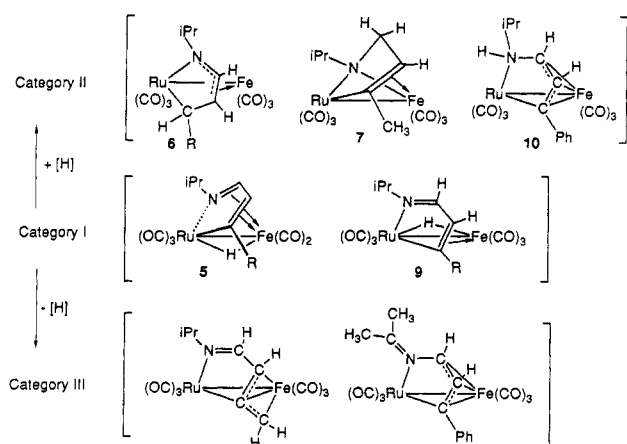


Figure 9. Coordination modes of the monoazadienyl ligand encountered in  $\text{FeRu}$ -carbonyl complexes.

complex 7 is not fluxional on the NMR time scale. Obviously there is a strong preference of the  $\eta^2(\text{C}=\text{C})$  bond to be attached to Fe instead of to Ru. From the chemical shift of  $\text{C}_\alpha/\text{H}_\alpha$  and  $\text{C}_\beta$  in the NMR spectra it can be concluded that the  $\pi(\text{C}=\text{C})$  bond is linked to Fe. As compared to the  $\text{Ru}_2$  system, the resonance of  $\text{C}_\alpha$  has

shifted to high frequency by only 2.2 ppm. The resonances of  $\text{H}_\alpha$  and  $\text{C}_\beta$ , however, experienced a low-frequency shift of 0.27 and 7.6 ppm, respectively. Such a difference in chemical shift would hardly be expected for the isomer of 7 featuring  $\pi$  coordination to Ru and has therefore been assigned to  $\pi$  coordination to Fe. Complex 10aI also shows a few interesting aspects. Its spectroscopic data are in complete agreement with the data found for the  $\text{Ru}_2$  analogue.<sup>4d</sup> The most profound differences in NMR chemical shifts, caused by the influence of Fe, have been found for  $\text{H}_\alpha$  (0.27 ppm low-frequency shift) and  $\text{C}_{\text{im}}$  (9.1 ppm high frequency). Most remarkable, however, is the stereochemistry. Complex 10 features two chiral centers, the cyclometalated Ru atom and the N atom,<sup>15a</sup> and therefore it may exist in two diastereomeric forms. Via the synthetic method, outlined before, complex 10a has been formed with 100% diastereoselectivity.<sup>15b</sup>

The complexes 6a,b fall within category II as well and thus possess a reduced metallacycle, bearing the extra hydrogen at  $\text{C}_\beta$ . This coordination mode is unprecedented and has therefore been ascertained by an X-ray structure determination of 6a (*vide supra*). In principle, the structure of 6 may be represented by the two mesomeric forms A and B (Figure 10). Structure A contains an amido

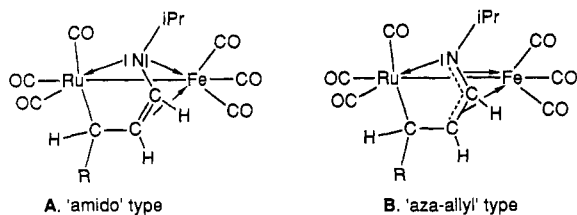


Figure 10. Two mesomeric structures of complex 6.

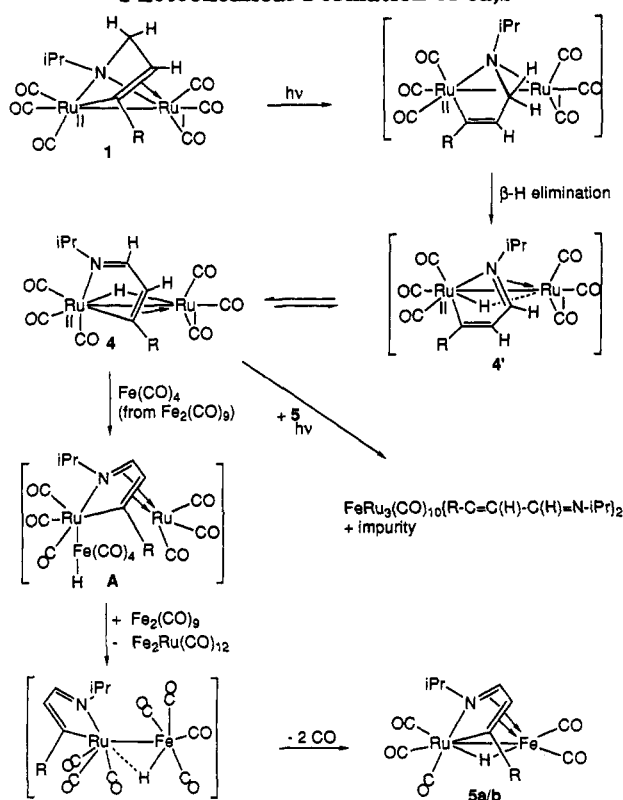
bridge coupled to a  $\sigma$ -allylic unit, which is  $\pi$  coordinated to Fe. Such a coordination mode is the theoretical prediction of the ultimate reduction of a  $\pi$ -bonded diene ligand and has been reported recently for a mononuclear  $ZrCp_2$ -MAD complex.<sup>26a</sup> In structure B the double bond of the  $\sigma$ -allylic moiety is delocalized to the amido bridge, thus forming a  $\eta^3$ -azaallylic unit. The latter interpretation (B) fits best the solid-state structure and is also in better agreement with the spectroscopic data than the structure of mesomer A. The NMR resonances of the azaallylic part are very similar to the related part of the ligand system in the azaallyl complex  $Ru_2(CO)_6\{RC(H)_2CC(H)NR\}$  (Figure 1).<sup>4a</sup> The resonances of  $H_{im}/C_{im}$  in 6 have been found between 6.5 and 7.0 ppm and between 107 and 110 ppm, respectively, which is comparable to the corresponding values of 6.9/108–109 ppm for the  $Ru_2$  complex. Like the isomeric complex 10, the complexes 6a,b possess two centers of chirality, one at the Ru atom and one at  $C_\beta$ .<sup>15a</sup> In the NMR spectra, however, only one diastereomer has been observed. The difference in chemical shift of  $H_\beta$  between 6a and 6b (3.41 and 2.02 ppm, respectively) should be attributed to mesomeric or inductive effects of the substituents.<sup>26b</sup>

## Discussion

**Formation of  $HFeRu(CO)_5\{RC=C(H)C(H)=N-iPr\}$  (5a,b).** The synthesis of the complexes 5a,b via the photochemical reaction of  $Ru_2(CO)_6\{RC=C(H)CH_2N-iPr\}$  (1a,b) with  $Fe_2(CO)_9$  has been reported previously.<sup>5</sup> A byproduct in this reaction was the complex  $FeRu_3(CO)_{10}\{RC=C(H)C(H)=N-iPr\}_2$ . Unfortunately, this compound could not be obtained in a pure state and could only be identified by FD mass spectrometry and IR.<sup>5</sup> The identity of the heteronuclear compound has been verified by an additional reactivity test with  $H_2$ , resulting in the formation of  $H_4Ru_4(CO)_{12}$  and 5a,b. The presence of  $FeRu_3(CO)_{10}\{RC=C(H)C(H)=N-iPr\}_2$  as one of the reaction products provided a key to the mechanism of the reaction of 1 with  $Fe_2(CO)_9$ . Most probably  $FeRu_3(CO)_{10}\{RC=C(H)C(H)=N-iPr\}_2$  is formed by dimerization of a  $HFeRu$  and a  $HRu_2$  complex, such as 4, by loss of  $H_2$ , by analogy with the formation of  $Ru_4(CO)_{10}\{RC=C(H)C(H)=N-iPr\}_2$  (3) (Figure 2). The intermediate complex  $HRu_2(CO)_6\{RC=C(H)C(H)=N-iPr\}$  (4) might originate from 1 by the mechanism depicted in Scheme I.

An open coordination site may be created on  $Ru_I$  either by the photochemical cleavage of the  $\pi(C=C)$  coordination or by the dissociation of a CO ligand. The same question also played a role in the photochemical conversion of  $Fe(CO)_3(\eta^4\text{-polyene})$  into  $HFe(CO)_2(\eta^5\text{-polyene})$  complexes,

## Scheme I. Proposed Mechanism for the Photochemical Formation of 5a,b



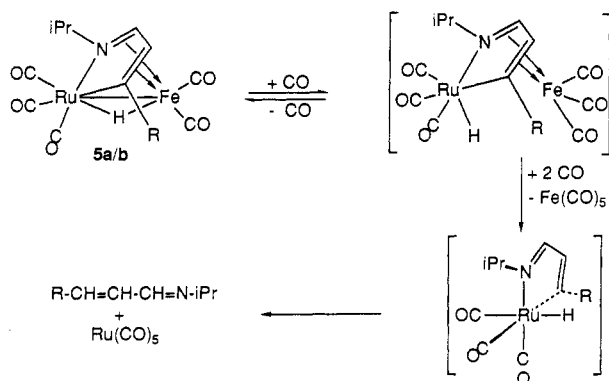
which are isolobally related to 1 and 5, respectively.<sup>27</sup> In that case the CO-dissociation pathway was considered as the most important, although the hapticity change of the polyene ligand could not be discounted. In our case the breaking of the  $\pi(C=C)$  coordination seems more likely, because filtered light with  $\lambda > 300$  nm has been used and the MLCT ( $M \rightarrow \pi^*(CO)$ ) transition probably lies in the UV region. A second reason may be found in the analogy with the reaction of 3 with  $CO$ ,<sup>4e</sup> where the product formation could be explained by the photochemically induced selective breaking of the  $Ru-\pi(C=C)$  bond, while the selective breaking of the  $Ru-\pi(C=N)$  bond was believed to occur thermally.

After creation of the open site on  $Ru_I$ , a  $\beta$ -H elimination reaction may take place, involving one of the methylene C-H bonds. This reaction results in the  $Ru_2$ -hydrido complex 4', in which the monoazadienyl ligand is  $\eta^2(C=N)$ -bonded to  $Ru_I$ . This complex is likely to rearrange to the more stable isomer 4, having the olefinic part of the monoazadienyl ligand  $\pi$ -bonded to  $Ru_I$ . From this stage of the reaction two pathways may be followed. The hydrido complex 4 may react with  $Fe_2(CO)_9$ , involving an oxidative addition of the  $Ru_{II}-H$  bond (4 possesses a bridging hydride<sup>4d</sup>) to an  $Fe(CO)_4$  unit delivered by  $Fe_2(CO)_9$ . Such a type of reaction is known in the literature, where it is also used for the preparation of heteronuclear complexes.<sup>28</sup> In the resulting intermediate A the  $Ru-Ru$  bond must be broken to afford a closed valence shell situation. This means that the  $Ru_I(CO)_3$  unit is only  $\pi(C=C)$ - and  $\pi(C=N)$ -bonded, which interaction is comparable to the bonding in the monomeric complex

(26) (a) Davis, J. M.; Whitby, R. J.; Jaza-Chamiec, A. *J. Chem. Soc., Chem. Commun.* 1991, 1743. (b) In theory this difference in chemical shift for  $H_\beta$  between 6a and 6b could also be due to the presence of two different diastereomeric forms of either complex. However, in view of the mechanism of formation via intermediate complex 9 (see Scheme II) this is unlikely.

(27) Astley, S. T.; Churton, M. P. V.; Hitam, R. B.; Rest, A. J. *J. Chem. Soc., Dalton Trans.* 1990, 3243.

(28) Kovacs, I.; Sisak, A.; Ungvary, F.; Marko, L. *Organometallics* 1989, 8, 1873.

**Scheme II. Proposed Mechanism for the Reductive-Elimination Reaction of 5a,b**


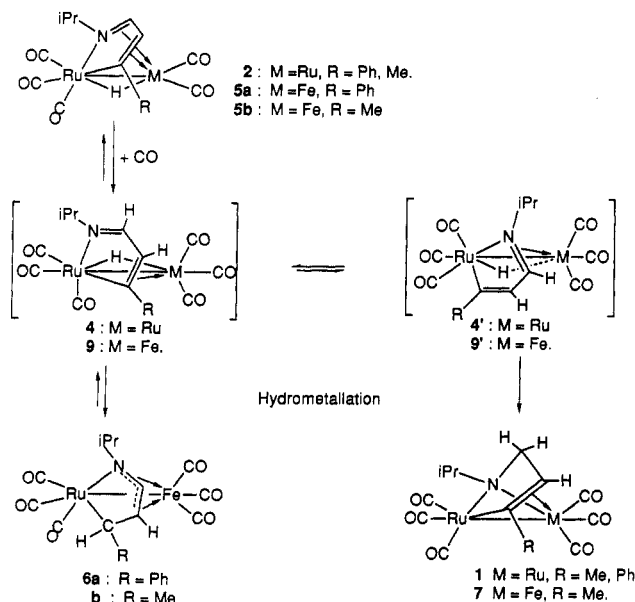
$\text{Ru(CO)}_3(\pi, \pi\text{-MAD})$  and can be expected to be accordingly weak.<sup>29</sup> Therefore, the  $\text{Ru}_1(\text{CO})_3$  unit is likely to be abstracted by  $\text{Fe}_2(\text{CO})_9$ , yielding the byproduct  $\text{Fe}_2\text{Ru(CO)}_{12}$  and  $\text{HFe(CO)}_4\text{Ru(CO)}_3\{\text{RC}=\text{C(H)C(H)=N-iPr}\}$ . The latter complex may rapidly react either photochemically or thermally to **5a,b** by substitution of two CO ligands on Fe by the  $\pi$  system of the monoazadienyl ligand.

The second route starting from complex **4** is the reaction with a molecule of complex **5**, formed *via* the first route, which by loss of  $\text{H}_2$  gives  $\text{FeRu}_3(\text{CO})_{10}\{\text{RC}=\text{C(H)C(H)=N-iPr}\}_2$ .

Part of the mechanism in Scheme I can be rationalized by the separate examination of the reaction of complex **4** with  $\text{Fe}_2(\text{CO})_9$ . Because no general and high-yield route to **4** was known, first a new synthesis of **4** was developed. For this purpose the purple butterfly complex  $\text{H}_2\text{Ru}_4(\text{CO})_8\{\text{RC}=\text{C(H)C(H)=N-iPr}\}_2$  was taken as starting material. The thermal reaction of this tetranuclear complex with CO, yielding complex **1**, has been reported earlier.<sup>4d</sup> When this reaction was performed under milder reaction conditions, i.e. photochemically, quantitative formation of **4** was effected. Complex **4** reacted with  $\text{Fe}_2(\text{CO})_9$  already at room temperature in the dark, and complexes **5a,b** could be isolated afterward in high yield. These findings are in agreement with the mechanism as proposed in Scheme I.

**Reactivity of 5a,b toward CO.** From the reaction sequence of  $\text{Ru}_3(\text{CO})_{12}$  with MAD (Figures 1 and 2) it has become clear that under thermal conditions hydrido complexes are not reaction products. Only products in which the hydrogen atoms are located on the  $\text{C}=\text{C}-\text{C}=\text{N}$  skeleton were isolated. In order to test if the hydride in **5a,b** could be returned to the monoazadienyl ligand as well and what the influence of heteronuclearity on the product distribution would be, the reactivity of **5a,b** toward CO under mild and thermal conditions was probed.

The product formation on the heteronuclear metal core turned out to be different indeed, and the main line of events occurring has been outlined in Schemes II and III. The results of the reaction of **5a,b** with CO indicate that two pathways may be followed. The hydride ligand is placed back on the monoazadienyl ligand, reducing either the metal or the monoazadienyl ligand. The attack of **5a,b** by CO may be rationalized by assuming a different initial reaction step for each of these pathways. The reductive-elimination pathway may start by the opening of the hydride bridge, while the beginning of the ligand

**Scheme III. Proposed Mechanism for the Ligand Reduction of 5a,b or 2 under CO**


reduction mechanism involves substitution of the  $\pi(\text{C}=\text{N})$  coordination to Fe by CO. Both pathways will be discussed now in more detail.

**Reductive-Elimination Pathway.** The reductive-elimination pathway, as observed for **5b** in the reaction with CO at 20 °C, requires opening of the hydride bridge (Scheme II). Unfortunately, the bridging position of the hydride in **5b** could not be ascertained by X-ray diffraction,<sup>5</sup> but the bridging character of the hydride has been corroborated by the negative  $\text{CCl}_4$  test<sup>5</sup> (terminal hydrides generally exchange rapidly with a Cl atom of  $\text{CCl}_4$ ) and also by the magnitude of the  $^{13}\text{C}-^1\text{H}$  coupling constants, measured in the carbonyl part of the proton-coupled  $^{13}\text{C}$  spectrum of **5a,b**.<sup>30</sup>

The added CO ligand will induce the hydride to move to a terminal position at Ru (Scheme II), concomitantly breaking the metal-metal bond in order to obtain a closed valence shell situation. The resulting intermediate is very similar to the trinuclear intermediate in Scheme I. The next step is substitution of the  $\pi$  bonds to Fe by CO, yielding  $\text{Fe(CO)}_5$  and a mononuclear Ru-hydrido complex. This intermediate is unstable at room temperature,<sup>29a</sup> probably yielding  $\text{Ru(CO)}_3(\eta^4\text{-MAD})$  first, which is not stable under a CO atmosphere either.<sup>4a</sup> The  $\pi$ -complexed MAD ligand will be substituted to afford the observed reaction products  $\text{Ru(CO)}_5$  (or  $\text{Ru}_3(\text{CO})_{12}$ ) and the original ligand MAD.

At room temperature the reaction sequence in Scheme I takes place only for complex **5b**. For **5a**, bearing an aromatic R substituent, the bridge-opening process is not observed at room temperature, even after 48 h. The  $^{13}\text{C}-^1\text{H}$  coupling constants at the carbonyl resonances, being exactly the same for both **5a** and **5b**,<sup>26</sup> indicate that the hydride ligands in both complexes are in similar positions,

(30) Carbonyl resonances (in ppm;  $J$  in Hz) of the proton-coupled  $^{13}\text{C}$  spectra (75.46 MHz, 20 °C,  $\text{C}_6\text{D}_6$ ) of **5a,b**: complex **5a**, 215.0 (d, 7.0), 212.9 (d, 7.6), 195.0 (d, 3.2), 191.6 (d, 13.7), 190.7 (d, 2.3); complex **5b**, 215.7 (d, 7.0), 214.9 (d, 7.9), 196.7 (d, 3.5), 192.4 (d, 18.5), 190.8 (d, 3.5). The coupling patterns for **5a** and **5b** are very alike and are in support of a bridging character for the hydride. Coupling constants for the  $\text{Fe}-\text{CO}$ 's of 7 Hz are typical for cis coupling. The two small cis coupling constants ( $\pm 3$  Hz) and one large trans coupling constant ( $\pm 18$  Hz) for the  $\text{Ru}-\text{CO}$ 's indicate that the hydride is indeed in a bridging position.

(29) (a) Beers, O. C. P.; Bouman, M. M.; Elsevier, C. J.; Smeets, W. J. J.; Spek, A. L. *Inorg. Chem.*, in press. (b) Otsuka, S.; Yoshida, T.; Nakamura, A. *Inorg. Chem.* 1967, 6, 20.

so their different reactivity is unlikely to be caused by a structural difference of the hydride bridge. More likely, the primary intermediate in Scheme II is much more stable for **5a** than for **5b**, thus allowing the back-reaction to take place. This seems reasonable, because also mononuclear  $\text{Fe}(\text{CO})_3(\eta^4\text{-MAD})$  complexes with aromatic substituents exhibit enhanced stability compared to aliphatic substituted ones.<sup>29</sup>

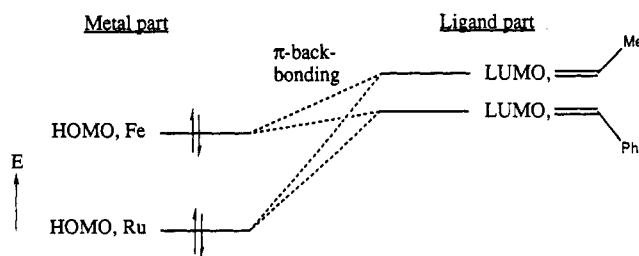
**Ligand-Reduction Pathway.** At higher temperatures the other reaction pathway, in which the ligand is reduced, becomes possible, and a mechanism as shown in Scheme III is proposed. This mechanism should explain the observed influence of both the R substituent and the metal on the reactivity of  $\text{HMRu}(\text{CO})_5\{\text{RC}=\text{C}(\text{H})\text{C}(\text{H})=\text{N-iPr}\}$  toward CO. To summarize the observed product formation, a selective hydride transfer to  $\text{C}_\beta$  occurred in the case of  $\text{M} = \text{Fe}/\text{R} = \text{Ph}$ , while for  $\text{M} = \text{Ru}$  the reaction appeared to be independent of the R group and is characterized by a selective transfer of the hydride to  $\text{C}_{\text{im}}$ . In the case of  $\text{M} = \text{Fe}/\text{R} = \text{Me}$ , there is no selectivity and both  $\text{C}=\text{C}$  and  $\text{C}=\text{N}$  reduction takes place, resulting in the formation of both **6b** and **7**.

The first step in the mechanism of ligand reduction probably is the substitution of the  $\pi(\text{C}=\text{N})$  coordination by CO, resulting in the intermediates **4/9**. This step takes place already at room temperature in the homonuclear case (i.e. conversion of **2** to **4**).<sup>4d</sup> The assumption that the heteronuclear complex **9** acts as a reaction intermediate has been rationalized in two ways. First, we have been able to synthesize **9a** (*vide supra*), which under a CO atmosphere (under conditions even milder than were used for **5a,b**, *viz.* 70 °C instead of 100 °C) gave quantitative conversion into **6a**. A second indication was obtained from the photochemical back-reaction of **6a** into **5a** under a CO atmosphere, when small amounts of complex **9a** could be observed in the IR spectrum of the resulting reaction mixture.

From the stage of the intermediate **4/9** a hydrometalation step, i.e. an insertion of the  $\pi(\text{C}=\text{C})$  bond in the Fe-H bond, directly accounts for the formation of **6**. The formation of **1** and **7**, however, requires an equilibrium between **4/9** and **4'/9'**. In the latter only the  $\text{C}=\text{N}$  bond is  $\pi$ -coordinated. Hydrometalation from that stage then results in reduction of the  $\text{C}=\text{N}$  bond and formation of **1/7**. Therefore, the crucial part in the mechanism in Scheme III is represented by the equilibrium between the intermediates **4/9** and **4'/9'**. The strength of the  $\pi(\text{C}=\text{C})$  coordination in **4/9** is of pivotal importance for the position of that equilibrium. The influence of the metal (Fe or Ru) and the R substituent (Ph or Me) on the strength of the  $\pi(\text{C}=\text{C})$  coordination in **4/9** will be discussed now.

The dependence of the strength of  $\pi(\text{C}=\text{C})$  coordination on the metal and on the R group can best be explained by qualitative frontier orbital considerations (Figure 11), based on general conclusions obtained from theoretical calculations.<sup>31,32</sup>

The HOMO of the Ru unit may be expected to be at a lower energy than that of the isoelectronic Fe fragment, due to a smaller d-d electron repulsion in the more diffuse 4d orbitals of Ru.<sup>31</sup> Due to the relative lowering of the



**Figure 11.** Qualitative frontier orbital diagram with relevant bonding interactions.

HOMO of Ru as compared to Fe, the  $\pi$  back-donation contribution to the  $\text{C}=\text{C}$  bond will decrease and the interaction will be weakened in the case of the homodinuclear Ru complex **4**. With regard to the influence of the R substituent, the introduction of an electron-donating substituent on a diene frame in general will raise both the energy of the HOMO and the LUMO of the diene.<sup>32</sup> Introduction of additional conjugation, as is the case with a Ph substituent, will also raise the energy level of the HOMO but lower the energy of the LUMO.<sup>32</sup>

On the basis of Figure 11, the  $\pi$  back-bonding in the  $\text{M}-\pi(\text{C}=\text{C})$  interaction may be expected to be the largest for  $\text{M} = \text{Fe}$  and  $\text{R} = \text{Ph}$  (**9a**). A slightly weaker interaction will result in the case of  $\text{M} = \text{Fe}$ ,  $\text{R} = \text{Me}$ , due to an energy increase of the LUMO of the diene fragment. Further weakening of the  $\pi$  coordination occurs when Fe is replaced by Ru, due to a lowering of the HOMO of the metal fragment.

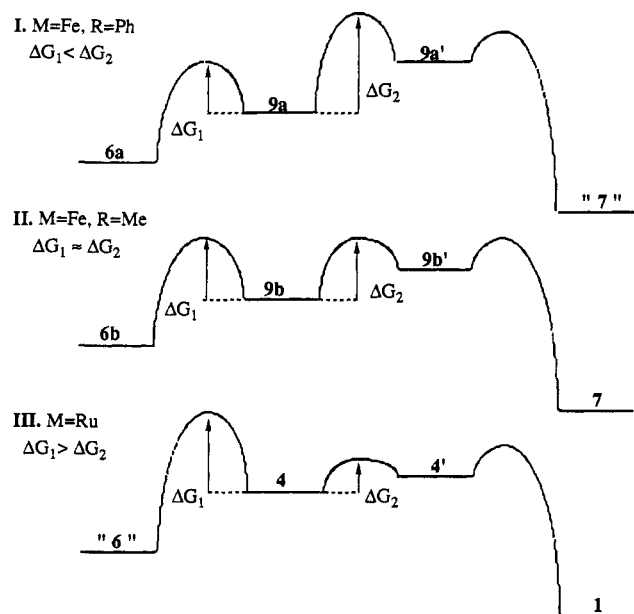
On the basis of the qualitative picture in Figure 11 the formation of **6a** may be readily rationalized. A very strong coordination of the  $\pi(\text{C}=\text{C})$  bond in **9a**, which is in agreement with the extreme lengthening of the  $\text{C}(5)-\text{C}(6)$  bond in **9a** (Figure 8), precludes the transformation of **9a** into **9a'**, and therefore hydrometalation takes place in intermediate **9a**. However, the reduced  $\pi$  back-bonding in the  $\text{M}-\pi(\text{C}=\text{C})$  fragment in the case of **4** and **9b** as compared to **9a** clearly allows equilibrium with **4'** and **9'**, respectively, and so the formation of **1** and **7** becomes possible.

For a better understanding of the reactions taking place within this system a qualitative energy profile as a function of the reaction coordinate has been formulated (Figure 12). In profile I, concerning the heteronuclear system with  $\text{R} = \text{Ph}$ , the activation energy barrier  $\Delta G_1$  from **9a** to **9a'** is higher than the barrier  $\Delta G_2$  from **9a** to **6a**. Thus, selective reduction of the  $\text{C}=\text{C}$  bond occurs, yielding **6a**. In the heteronuclear case with  $\text{R} = \text{Me}$  (profile II) the energy level of complex **9b** increases with respect to profile I, due to the weakening of the  $\pi(\text{C}=\text{C})$  interaction. Now the activation barriers  $\Delta G_1$  and  $\Delta G_2$  become of comparable magnitude, allowing both processes. Because in this case there is not a single product due to a kinetic control of the reaction, we were able to verify the relative thermodynamic stability of both products. Under the conditions of its formation product **6b** appeared to be converted slowly into the thermodynamically more favorable complex **7** (and to **1**, but this is a result of the irreversible reductive elimination pathway; see Scheme II). For the homodinuclear  $\text{Ru}_2$  complexes (profile III)  $\Delta G_2$  is considerably smaller than  $\Delta G_1$ , thus giving rise to the both kinetically and thermodynamically favored complex **1**.

**Stereochemistry of the Formation of 6.** Some attention should be given to the stereochemistry of the formation of **6**. The starting complexes **5** and **9** are chiral

(31) Ziegler, T.; Tschinke, V.; Ursenbach, C. *J. Am. Chem. Soc.* 1987, 109, 4825.

(32) Fleming, I. *Frontier Orbitals and Organic Chemical Reactions*; Wiley: London, 1976; p 120.



**Figure 12.** Qualitative energy profiles for the reaction of  $\text{HMRu}(\text{CO})_5\{\text{RC}=\text{C}(\text{H})\text{C}(\text{H})=\text{N}-i\text{Pr}\}$  with CO.

and exist as racemic mixtures of both enantiomers. In the product a new chiral center is formed at  $\text{C}_\beta$ , but this process is completely governed by the chirality already present; therefore, the formation of **6** takes place with complete diastereoselectivity. When we examine the crystal structures of both **9a** and **6a** (Figures 7 and 8), which are the starting complex and product of the hydride transfer reaction, respectively, this diastereoselectivity may be readily understood. The hydride must always approach  $\text{C}_\beta$  from the Fe side, because in the conversion from **9** into **6** insertion of the  $\pi(\text{C}=\text{C})$  bond into the Fe-H bond takes place. Probably, this regioselectivity is responsible for the observed diastereoselectivity. The X-ray structure of **6a** also allows the formal definition of the stereochemistry of **6a**, being a mixture of the enantiomers  $\text{R}_{\text{C}(\beta)}\text{C}_{\text{Ru}}\text{A}_{\text{Fe}}$  and  $\text{S}_{\text{C}(\beta)}\text{A}_{\text{Ru}}\text{C}_{\text{Fe}}$ .<sup>33</sup>

**Interconversions between the FeRu Complexes.** A number of the above-mentioned complexes appear to be interconvertible. The reaction of **5a,b** with CO to yield **6a,b** is reversible, which can be brought about either thermally or photochemically. The conversions of **6a,b** into **5a,b** provide nice examples of C-H activation. Especially the photochemical process is interesting, because of the mild reaction conditions under which the C-H activation process takes place. Probably the role of light is to break the  $\eta^3$ -azaallyl coordination, thereby creating an open site, which is a prerequisite for C-H activation. In the resulting intermediate the azaallyl moiety then is bonded in an  $\eta^1$  fashion via the nitrogen atom. After C-H activation the  $\pi$ -electrons of the ligand system are redistributed and complex **9** is formed, as we were able to show by IR spectroscopy in the case of **9a**. The thermal reactivity of **9a** is dependent on the presence of CO. As

was already indicated above, **9a** was converted into **6a** quantitatively under an atmosphere of CO. Without CO, compound **9a** could be converted into **5a** also quantitatively, either under thermal or under photochemical conditions.

Finally, the thermal reactivity of complex **10a** was tested, but **10a** appeared to be thermally inert. No conversion into the other diastereomer has been observed.

**Comparison of the Reactivity of Homonuclear  $\text{Ru}_2$ -Monoazadienyl Complexes with That of Their Heteronuclear FeRu Analogues.** From the comparative study of the  $\text{Ru}_2$  and FeRu analogues **2** and **5** (*vide supra*) and their reactivity toward CO, it could be concluded that  $\pi$  coordination of the monoazadienyl  $\pi$  system to Fe is much stronger than to Ru. This phenomenon has been shown most illustratively by comparison of the reaction of **5a** and **2a** with CO at room temperature. In the  $\text{Ru}_2$  case very fast substitution of the  $\pi$ -imine interaction is observed, whereas no reaction takes place in the FeRu system. The question of the strength of the  $\pi$ -interaction to Fe compared to Ru has also been under study in the case of the reactivity of  $\text{MM}'(\text{CO})_6(\text{R-DAB})$  toward alkynes.<sup>2</sup> The observed reactivity in those complexes, however, was explained by the assumption that the Fe- $\pi(\text{C}=\text{N})$  bond was weaker than the Ru- $\pi(\text{C}=\text{N})$  interaction because of an obviously greater amount of  $\pi$  backbonding in the Ru case. One observation, which could not be satisfactorily explained, was that in the case of the heterodinuclear complex  $\text{FeRu}(\text{CO})_6(\text{R-DAB})$  only the isomer could be obtained with the  $\eta^2(\text{C}=\text{N})$  coordination to Fe, irrespective of the way the complex was synthesized. In our study we also encountered an example showing the preference of  $\pi$  coordination to Fe over Ru, which can be explained on the basis of Figure 11. This example concerns complex **7**, which shows a strong preference for  $\pi$ -coordination of the olefinic bond to Fe, whereas the homonuclear analogue **1** is fluxional.

The general conclusion from this study is that  $\pi(\text{C}=\text{C})$  and  $\pi(\text{C}=\text{N})$  interactions to Fe are stronger than those to Ru, which finding may be important for the development of catalysts that take part in, for example, hydrogenation or hydroformylation processes of unsaturated substrates. The coordination strength of the unsaturated substrate to the metal center which is involved may play a role in determining the rate and selectivity of the reaction under study. Finally, the reaction of complexes **2** and **5** with CO may be considered as an elegant model system for the study of chemoselective hydrogenation of C=C and C=N moieties.

**Acknowledgment.** The crystallographic part of this work was supported by the Netherlands Foundation for Chemical Research (SON) with financial aid from the Netherlands Organization for Scientific Research (NWO). We are indebted to A. J. M. Duisenberg for the X-ray data collection and to Prof. Dr. K. Vrieze for his support and his interest in the subject.

**Supplementary Material Available:** ORTEP plots and tables of hydrogen atom parameters, anisotropic thermal parameters, bond distances and bond angles for **6a** and **9a** (10 pages). Ordering information is given on any current masthead page.

OM920707X

(33) The absolute configuration of chiral metal centers has been denoted by following the Brown-Cook-Sloan modification of the CIP rules.<sup>34</sup>

(34) (a) Brown, M. F.; Cook, B. R.; Sloan, T. E. *Inorg. Chem.* 1975, 14, 1273. (b) IUPAC. *Nomenclature of Inorganic Chemistry, Recommendations 1990*; Leigh, G. J., Ed.; Blackwell: Oxford, England, 1990; pp 171, 186.